Vectored Immunoprophylaxis and Treatment of SARS-CoV-2 Infection

Takuya Tada[1], Belinda M. Dcosta[1], Julia Minnee[1] and Nathaniel R. Landau[1]

Affiliation:

[1]Department of Microbiology, NYU Grossman School of Medicine, New York, NY, USA.

#Corresponding author:

Nathaniel R. Landau, Ph.D.

NYU Grossman School of Medicine

430 East 29th Street, Alexandria West Building, Rm 509, New York, NY 10016

Email: nathaniel.landau@med.nyu.edu

Phone: (212) 263-9197

19 **Summary**

20 Vectored immunoprophylaxis was first developed as a means to establish engineered immunity

21 to HIV through the use of an adeno-associated viral vector expressing a broadly neutralizing

22 antibody. We have applied this concept to establish long-term prophylaxis against SARS-CoV-2

23 by adeno-associated and lentiviral vectors expressing a high affinity ACE2 decoy receptor.

24 Administration of decoy-expressing AAV vectors based on AAV2.retro and AAV6.2 by intranasal

25 instillation or intramuscular injection protected mice against high-titered SARS-CoV-2 infection.

26 AAV and lentiviral vectored immunoprophylaxis was durable and active against recent SARS-

27 CoV-2 Omicron subvariants. The AAV vectors were also effective when administered up to 24

28 hours post-infection. Vectored immunoprophylaxis could be of value for immunocompromised

29 individuals for whom vaccination is not practical and as a means to rapidly establish protection

30 from infection. Unlike monoclonal antibody therapy, the approach is expected to remain active

31 despite continued evolution viral variants.

Introduction

The concept of vectored immunoprophylaxis was first proposed as an approach to establish protection against HIV infection by the vectored expression of a broadly neutralizing antibody[1], replacing the need to derive a vaccine immunogen capable of eliciting such antibodies. The approach has since been found to be effective as a therapeutic approach to suppressing virus replication the nonhuman primate SIV model using adeno-associated viruses (AAV) vectors expressing broadly neutralizing antibodies and is currently in clinical trials as a means to suppress HIV replication in infected individuals[2,3].

Vectored immunoprophylaxis for SARS-CoV-2 through the expression of neutralizing monoclonal antibodies is problematic because of the extraordinarily rapid evolution of the virus. Monoclonal antibody therapy has been highly successful for the treatment of severe COVID-19, decreasing hospitalization and deaths[4] but has been largely sidelined by the extraordinarily rapid appearance of viral variants that escape neutralization. The first Omicron variant, BA.1, contained 34 mutations in the spike protein, most of which were within or close to the spike protein receptor binding domain and allowed for escape from most of the therapeutic monoclonal antibodies. The Regeneron REGN-COV2 cocktail, a cocktail of REGN10933 and REGN10987 monoclonal antibodies, and the Lilly LY-CoV555 potently neutralize the earlier variants of concern (Alpha, Beta, Gamma and Delta) but their IC_{50}s against the Omicron BA.1 variant was greatly increased[5-14]. Vir/GSK VIR-7831 (Sotrovimab) was thought to maintain neutralizing activity against Omicrons BA.1 and BA.2 but was later found to be 10.5- and 340-fold decreased in neutralizing activity against the variants[8-10,12,14,15]. Lilly LY-CoV1404 maintained neutralizing titer against BA.1, BA.2 and BA.4/5[16] but fails to neutralize the more recent, further mutated Omicron variants BQ1.1 and XBB[17]. The extraordinarily rapid evolution of the virus is likely to continue over the next several

3

56   years, imposing a challenge to the development of monoclonal antibodies from which the virus

57   cannot escape. The rapidity of virus evolution is also a challenge for the design of effective

58   vaccines.

59

60   A strategy to inhibit virus entry that is less subject to escape by novel variants is that of receptor

61   decoys. The strategy is based on soluble forms of the protein, fused to the Fc domain of an

62   immunoglobulin heavy chain to increase its half-life *in vivo*[18]. While viruses can mutate epitopes

63   in the spike protein driven by selective pressure to escape neutralization by antibodies elicited

64   from previous infection or vaccination, the spike protein needs to conserve high affinity binding to

65   its receptor, thereby preserving the neutralizing activity of the receptor decoy. Receptor decoys

66   were first developed as a therapeutic for HIV infection[19,20]. A recombinant protein consisting of

67   the ectodomain of CD4 fused to an immunoglobulin Fc domain was found to bind the viral

68   envelope glycoprotein gp120 with high affinity and potently neutralize the virus *in vitro* but in

69   clinical trials the protein showed no benefit. More recently, the concept was revived by Gardner

70   *et al.* who showed that an enhanced eCD4-Ig protected rhesus macaques from multiple

71   challenges with SIV[3].

72

73   Receptor decoys for SARS-CoV-2 based on soluble forms of ACE2 have been developed by

74   several groups[21-28]. We previously reported the development of a receptor decoy protein termed

75   an "ACE2 microbody" in which the ACE2 ectodomain is fused to the CH3 domain of a human

76   immunoglobulin IgG1 heavy chain Fc region[21]. The decoy proteins, administered by intranasal

77   (i.n.) instillation, have been shown in mouse and hamster models to protect from infection when

78   given shortly prior to infection and to therapeutically suppress virus replication when given up to

79   about 12 hours post-infection[29]. The introduction of point mutations into the ACE2 spike protein

80   binding region of the decoy to increased its affinity for the spike further increased the effectiveness

81   of the proteins[22,24,26].

82

83   Here, we applied vectored immunoprophylaxis to SARS-CoV-2 using AAV and lentiviral vector

84   vectors expressing a modified high affinity ACE2 microbody. AAV2.retro and AAV6.2 vectors,

85   administered either i.n. or by intramuscular (i.m.) injection, provided a high degree of protection

86   in ACE2 transgenic and Balb/c mouse models. The protection was long-lasting and was effective

87   against recent Omicron variants. The AAV vectors were also effective therapeutically when

88   administered shortly post-infection. The lentiviral vector-based decoy was also effective at

89   suppressing virus replication, providing protection that showed no sign of diminishing two months

90   after i.n. administration. Decoy vectored-immunoprophylaxis could be a highly useful means to

91   protect immunocompromised individuals for whom vaccination is less effective and could offer a

92   therapy that remains active against new variants as the emerge.

93   **Results**

94   **Decoy-expressing AAV vectors inhibit SARS-CoV-2 infection.**

95   To determine the feasibility of vectored prophylaxis for SARS-CoV-2, we constructed AAV vectors

96   expressing an ACE2 receptor decoy. The decoy, termed ACE2.1mb, is similar to the ACE2

97   microbody we previously reported[21] that consists of the ACE2 ectodomain fused to a single CH3

98   domain of an IgG1 heavy chain Fc domain **(Figure 1A)**. The protein has been modified by the

99   introduction of point mutations in the ACE2 spike protein binding region that were reported by

100   Chen *et al.* to increase affinity for the spike protein[22] and by the introduction of an H345A point

101   mutation that inactivates its catalytic activity[30]. The coding sequence was cloned into an AAV

102   vector containing a CAG promoter and virus stock was produced with AAV2.retro and AAV6.2

103   capsids. AAV2 and AAV6 are reported to have tropism for cells of the mouse and human lung

104   and airway[31-33]. AAV2.retro is a variant of AAV2 that was selected for increased tropism for the

105   central nervous system (CNS) and retrograde movement in axons[34,35]. It has not been reported

106   to transduce lung cells but in pilot experiments, we found that it worked surprisingly well (not

107   shown). AAV6.2 is a variant of AAV6 that contains a single F129L mutation that was found to

108   increase the efficiency of mouse and human airway cell transduction[36]. The ability of the vectors

109   to protect cells from SARS-CoV-2 infection was tested in the lung cell-line A549.ACE2 and the

110   microglial cell-line CHME3.ACE2. The cells were transduced with serial dilutions of the decoy

111   vectors and then challenged 5 days later with D614G, BA.1, BA.2, BA.2.75, BA.4/5 and BQ.1

112   spike protein-pseudotyped lentiviruses carrying a luciferase reporter genome. At 2 days post-

113   infection (dpi), luciferase activity in the cultures was measured. The results showed that both

114   decoy-expressing AAVs protected A549.ACE2 and CHME3.ACE2 cells from infection (**Figure**

115   **1B**). Virus with the D614G spike was the most potently neutralized by the decoy while BA.2 was

116   the most resistant, with a 20-33-fold higher ID_{50} (defined as the multiplicity of infection (MOI) that

6

117   resulted in a 50% decrease in luciferase activity). The low ID_{50} required to block infection indicates

118   that the decoy was active on bystander cells and that it was not necessary to transduce all of the

119   cells in order to protect the culture.

120

121   The ability of the decoy-expressing vectors to inhibit SARS-CoV-2 live virus replication was tested

122   on A549.ACE2, CHME3.ACE2 and hSABCi-NS1.1 cells. The latter is a human small airway basal

123   cell-line grown in air-liquid interface culture conditions and differentiated into mature airway

124   epithelium cell-types the model the respiratory tract. The cells were transduced with decoy-

125   expressing or control GFP.nLuc AAV2.retro and AAV6.2 vectors and challenged a day later with

126   SARS-CoV-2 WA1/2020. Virus replication was measured by RT-qPCR quantification of cell-

127   associated viral RNA copies. The 3 cell-lines supported high levels of SARS-CoV-2 replication

128   (**Figure 1C left)**. Transduction of the CHME3.ACE2 cells with either of the AAV vectors resulted

129   in a 4-5 log decrease in viral RNA, a level that was not significantly higher than uninfected cells.

130   Transduction of the cells by the control AAV had no effect on SARS-CoV-2 replication. The results

131   in the A549.ACE2 cells were similar (**Figure 1C right)**. The vectors were also effective in the

132   hSABCi-NS1.1 human small airway basal cultures although the decrease was less pronounced

133   (50-100-fold) most likely because the cells did not support virus replication as high as in the other

134   cell-lines. The AAV6.2 vector was somewhat more effective than the AAV2.retro vector (**Figure

135   1D)**. Production of the decoy protein by the transduced CHME3.ACE2 and A549.ACE2 cells was

136   confirmed by pull-down of the protein from the culture supernatant on anti-His tag coated

137   magnetic beads and immunoblot analysis (**Figure 1E)**. The CHME3.ACE2 cells were found to

138   produce about 2-fold more decoy than A549.ACE2 which may have contributed to the greater

139   extent of protection in these cells. The concentration of the decoy protein in the culture medium

140   was 0.2-0.6 μg/ml, a concentration that was greater than the IC_{50} 0.15 μg/ml[21].

141

Vectored immunoprophylaxis *in vivo* by decoy-expressing AAV-vectors

143　The feasibility of vectored immunoprophylaxis for SARS-CoV-2 with the decoy-expressing AAV

144　vectors was tested in transgenic and non-transgenic mouse models. Decoy-expressing and

145　control GFP AAV2.retro and AAV6.2 vectors were administered to human ACE2 K18 transgenic

146　mice (hACE2 K18 Tg) i.n., i.v. or i.m. After 3 days, the mice were challenged with SARS-CoV-2

147　WA1/2020 and virus loads in the lung were measured 3-dpi **(Figure 2A)**. The results showed that

148　vector administration i.n. strongly suppressed virus replication in the mice, decreasing the virus

149　load by 5-logs, a level that was indistinguishable from uninfected mice (**Figure 2B**). The control

150　vectors had no effect on virus loads. Histology showed that the lungs of infected untreated mice

151　had prominent signs of interstitial pneumonia with thickened alveolar septa and inflammatory cell

152　infiltration while the lungs of decoy-expressing AAV vectors-treated mice showed no signs of

153　pneumonia and were free of infiltrating inflammatory cells (**Figure 2C**). The lungs of mice treated

154　with the decoy AAV vectors alone in the absence of SARS-CoV-2 infection were clear, indicating

155　that the decoy vectors themselves did not cause pulmonary inflammation (**Figure 2C**). Treatment

156　with the decoy vectors prevented the characteristic loss of body mass associated with untreated

157　SARS-CoV-2 infection (**Figure 2D**). A concern regarding vectored immunoprophylaxis is that the

158　decoy protein or the vectors themselves might induce inflammatory responses in the lungs;

159　however, analysis of proinflammatory and anti-inflammatory cytokine levels (IFNα, IL-10, TNFα,

160　IL12-p70, IL-6 and MCP-1) showed no induction of these cytokines following administration of the

161　vectors (**Figure S1**).

162

163　To test the effectiveness of the decoy vectors in protecting against the Omicron variants, Balb/c

164　mice, which support high level replication of SARS-CoV-2 Omicron variants through the

8

165   endogenous murine ACE2[37,38], were treated i.n. with decoy-expressing AAV or control AAV2.retro

166   or AAV6.2 vector and then challenged with Omicrons BA.1, BA.2 or BA.5. The results showed

167   that i.n. administration of decoy-expressing AAV vectors caused a dramatic decrease in virus

168   loads as compared to the control vectors (**Figure 2E**). The decoy-expressing vectors were most

169   effective against the BA.5 variant, decreasing the virus load 1,000-fold and least effective against

170   BA.2, decreasing virus load 100-fold (**Figure 2E**), a pattern that was similar to what was found

171   with the pseudotyped lentiviruses *in vitro*. Both AAV vectors were effective although the

172   AAV2.retro seemed to be slightly more suppressive against all three Omicrons. This conclusion

173   was confirmed in a dose-response analysis which showed that the decoy-expressing AAV2.retro

174   vector was about 10-fold more effective at virus load suppression. A 10,000-fold decrease in virus

175   load required 1×10^{10} vector genomes (vg) for AAV2.retro. The same degree of suppression by

176   AAV6.2 required 1×10^{11} vg (**Figure S2**).

177

178   Administration of the vectors i.n. delivered the vectors to the relevant organ but it was possible

179   that delivery by routes that targeted a different site in the body might also be effective given that

180   the decoy protein is stable *in vivo* and freely diffusible[29]. In support of this approach, i.m. delivery

181   of AAV-vectored immunoprophylaxis was effective for the suppression of SIV replication in the

182   macaque model[39]. We therefore tested the effectiveness of i.v. and i.m. administration of the

183   decoy-expressing AAV vectors **(Figure 2A)**. The results showed that i.m. administration was

184   highly effective, decreasing the virus load by 5-logs compared to control vector, a level that was

185   indistinguishable from uninfected mice (**Figure 2F**). I.v. administration was much less effective,

186   decreasing the virus load by only a 2-logs.

187

188   **Therapeutic use of vectored immunoprophylaxis for SARS-CoV-2**.

9

189   The studies described above tested the prophylactic effect of the decoy-expressing AAVs

190   administered prior to SARS-CoV-2 infection. It was possible that the approach might also be

191   effective therapeutically by administration post-infection. The effectiveness of administration post-

192   infection would depend on how soon post-infection they were administered and how fast the

193   vectors transduced lung cells and produced the encoded protein to establish an inhibitory

194   concentration in the respiratory tract. To determine this, we infected mice with SARS-CoV-2 and

195   then treated them at increasing times post-infection **(Figure 2G)**. The results showed that the

196   decoy-expressing vectors were effective when administered concomitant with SARS-CoV-2 and

197   up to 12 hours post-infection (**Figure 2G**). The treatment was partially effective at 24-hours and

198   lost efficacy at 48-hours. The results demonstrate remarkably rapid transduction and biosynthesis

199   of the decoy protein by the AAV vectors. While this time course would appear to be too short to

200   be of therapeutic use, the kinetics closely mirror what is seen in monoclonal antibody therapy of

201   SARS-CoV-2 in mouse models[1111118] suggesting that in humans, where the time-course of

202   disease is slower, the AAV vectors might act with the kinetics similar to that of highly effective

203   monoclonal antibodies.

204

205   **AAV decoy-expressing vectored immunoprophylaxis is highly durable.**

206   Although AAV does not integrate at a significant frequency into the host cell genome, the genome

207   remains stable in the host cell. In nonhuman primates and in clinical trials, AAV vectors have been

208   shown to maintain long-term expression of an encoded gene *in vivo*[40]. To test the durability of the

209   decoy-expressing AAV vectors, we constructed AAV2.retro and AAV6.2 vectors that expressed

210   a decoy-luciferase fusion protein. The vectors were administered i.n. to mice and the mice were

211   live-imaged over the next 30 days. Expression by both vectors in the lungs was first detected 24

212   hours post-treatment and then increased to maximal by day 3 **(Figure 3A)**. Expression levels

213   remained stable through day 14 after which they decreased slightly by day 30. Measurement of

214   luciferase activity in tissue homogenates further demonstrated durable expression by the vectors

215   (**Figure 3B**). The decoy proteins were readily detectable on day 1 and the following day,

216   expression increased 25-fold. To determine the durability of viral load suppression by the vectors,

217   mice were treated and then challenged with SARS-CoV-2 over a 30-day period. The results

218   showed that the decoy-expressing vectors strongly suppressed the virus loads of mice infected

219   that had been infected up to 30-days post-treatment (**Figure 3C**). Virus load suppression

220   appeared to begin to wane 30 days post-treatment but was still highly active, with the AAV2.retro

221   vector suppressing virus load nearly 1000-fold. The results were consistent with the slight

222   decrease in *in vivo* expression levels found for the decoy-luciferase fusion protein.

223

224   **Increased durability of vectored immunoprophylaxis with a decoy-expressing lentiviral**

225   **vector.**

226   The waning of protection established by the AAV vectors at 30 days led us to test whether a

227   different vector might be able to extend the durability protection. The use of an alternative vector

228   was also of interest in light of concerns about the possibly of pre-existing immunity to AAV in

229   some individuals noted in clinical trials[41]. Lentiviral vectors are generally not subject to pre-existing

230   immunity in humans. Moreover, because lentiviruses integrate into the host cell genome, the

231   vectors are maintained stably in the cell and in daughter cells that may be generated, allowing for

232   the possibility of long-term decoy expression and increased durability of protection. In addition,

233   pseudotyping of the vectors by VSV-G results in a broad target cell tropism. To test the feasibility

234   of lentiviral vectored immunoprophylaxis, we constructed a decoy-expressing lentiviral vector and

235   compared its effectiveness to the AAV vectors. Transduction of A549.ACE2 and CHME3.ACE2

236   cells with the vector showed that it expressed the decoy protein at a level similar to those of the

237   AAV vectors as measured in the supernatant pull-down assay (**Figure S3**). To determine the

238   potency of the protection, the cell-lines were transduced with a serial of the decoy-expressing

239   lentiviral vector and then challenged with the D614G and Omicron spike protein-pseudotyped

240   reporter viruses. The results showed that vector was highly protective against all of the variants

241   (**Figure 4A**). Overall, the potency of virus neutralization, calculated by the MOI required to

242   decrease infection by 50%, was very similar to that of the AAV vectors. As for the AAV vectors,

243   BA.2 was the most resistant to neutralization (8-fold in CHME3.ACE2 and 5.8-fold in A549.ACE2)

244   (**Figure 4A, below**). The ability of the vectors to neutralize the viruses at low MOIs confirmed that

245   only a small fraction of the cells needed to be transduced to protect the entire population.

246

247   To determine whether the decoy-expressing lentiviral vector could establish vectored

248   immunoprophylaxis, the vector was administered i.v. or i.n. and after 7 days, the mice were

249   challenged with WA1/2020 or Omicron BA.1. Virus loads in the lung were quantified 3-dpi (**Figure**

250   **4B, left**). In mice challenged with WA1/2020, i.v. injection resulted in a nearly 5-log decrease in

251   virus load while administration i.n. further decreased the virus load to undetectable levels **(Figure**

252   **4B, middle)**. The analysis of proinflammatory and anti-inflammatory cytokine levels (IFNα, IL-10,

253   TNFα, IL12-p70, IL-6 and MCP-1) showed that administration of the lentiviral vector had no

254   significant effect on the levels of these cytokines (**Figure S1**). A dose-response analysis in which

255   mice were administered decreasing amounts of the vector i.v. or i.n. confirmed the great efficacy

256   of i.n. administration; at a dose of 1 X 10^6 IU, virus loads were 100-fold lower in mice treated i.n.

257   compared to i.v. (**Figure S4**). Treatment with the vector also protected against Omicron BA.1 but

258   did not suppress virus replication to as great an extent, resulting in low level virus replication in

259   mice treated i.v. or i.n. To compare the protective effect of the vector with that of a therapeutic

260   monoclonal antibody, mice were administered the highly potent neutralizing monoclonal antibody

261   LY-CoV1404 by i.v. and i.n. routes and then infected with the Omicron BA.1 variant. The results

262   showed that the monoclonal antibody decreased the virus loads more effectively i.n. than i.v. but

263   was not as effective as the lentiviral vector **(Figure 4B, right)**. To test the durability of lentiviral

264   vectored immunoprophylaxis, mice were treated i.v. or i.n. with decoy-expressing or control GFP-

265   expressing lentiviral vector and challenged 7, 30 and 60 days later with SARS-CoV-2 WA1/2020.

266   The protection was found to persist over the 60-day time-course (**Figure 4C**). I.n. administration

267   of the vector caused a greater decrease in virus loads which interestingly, became even more

268   pronounced over time.

269

270   To understand the basis of the long-lasting protection provided by lentiviral vectored

271   immunoprophylaxis, we administered a GFP/luciferase-expressing lentiviral vector i.v. or i.n. and

272   determined the level of expression over the 60-day time-course by measuring luciferase activity

273   in cell lysates prepared from different tissues. The results showed that i.v administration resulted

274   in high level expression in the spleen at day-7 and moderate expression in the lungs and liver

275   (400-fold less in lung and 50-fold less in liver). The expression levels remained constant over the

276   time-course **(Figure 4D)**. There was no detectable expression in nasal tissue and trachea.

277   Administration of the vector i.n. resulted in high level expression in the lung, moderate levels in

278   the trachea (about 30-fold less on day 7) and nasal tissue. Levels in the spleen and liver were

279   undetectable. Expression levels remained constant at 30-days. At 60-days, expression in the lung

280   increased about 8-fold, a finding that could explain the increase in virus load suppression at this

281   time-point in mice treated by i.n. administration of the vector **(Figure 4C)**.

282

283   **Comparison of lung cell-types transduced by the AAV and lentiviral vectors**.

284   The effectiveness and longevity of the vectored immunoprophylaxis depends both upon the cell-

285   types and half-lives of the cells transduced by the vectors. To understand the basis of durable

286   protection, we characterized the cell-types transduced in the lung by the AAV and lentiviral

287   vectors. Mice were administered GFP-expressing AAV and lentiviral vectors i.n. and the GFP+

288   cells. The lungs were harvested 3 days later and the cells disaggregated. The cells were then

289   analyzed by flow cytometry using antibodies that distinguished various pulmonary cell-types. The

290   results showed that the majority of the cells transduced in the lungs by AAV2.retro and AAV6.2

291   were epithelial (79.5% and 94.2%, respectively) **(Figure 5A)**. Of the cells transduced by

292   AAV2.retro, 20.5% were leukocytes while AAV6.2 transduced fewer leukocytes (5.8%). Analysis

293   of the transduced leukocytes showed that the majority of cells were interstitial macrophages and

294   neutrophils with smaller proportions of T cells, B cells, DCs, monocytes and alveolar

295   macrophages. The distribution of leukocytes transduced by AAV6.2 was roughly similar. The

296   lentiviral vector targeted a larger proportion of leukocytes (57%). Of the transduced leukocytes,

297   the greatest proportion were DCs (26.3%) with substantial contributions from B cells (20.7%) and

298   monocytes (18.5%) **(Figure 5B)**. It is possible that the long-lasting expression by the lentiviral

299   vector resulted from the increased transduction of leukocytes, particularly of the DCs, as these

300   cells are thought to be long-lived residents in the lung[42].

14

Discussion

301 **Discussion**

302 Vectored prophylaxis was first developed as an approach to protect against HIV infection[1] in

303 which broadly neutralizing antibody was expressed in an AAV vector and was later expanded to

304 the use of an enhanced CD4-Ig fusion protein that established a high degree of resistance to SIV

305 infection in treated macaques[2,3]. We report here that that vectored expression of a high affinity

306 ACE2 microbody protein in which the ectodomain of ACE2 was mutated to increase its affinity for

307 the viral spike protein and inactivate catalytic activity fused to the CH3 domain of an IgG heavy

308 chain Fc[21] established a high degree of protection from SARS-CoV-2 in mouse models. Decoy-

309 expressing AAV2.retro and AAV6.2 vectors were both highly effective at establishing vectored

310 immunoprophylaxis in ACE2 K18 Tg and Balb/c mice. Mice treated with the decoy-expressing

311 AAV2.retro and AAV6.2 vectors were highly resistant to SARS-CoV-2 infection. Upon challenge

312 with high titered SARS-CoV-2 WA1/2020, viral RNA in the lungs 3-dpi was undetectable,

313 corresponding to a >10,000-fold decrease in virus loads; the lungs of the treated mice were free

314 of infiltrating leukocytes; there was no sign of pulmonary inflammation and the mice did not

315 experience the decrease in body weight that normally occurs in untreated or control vector-treated

316 mice. Delivery of the decoy by a lentiviral vector was as effective and appeared to be even more

317 durable. The vectors were well-tolerated; they did not disturb myeloid or lymphoid cell populations

318 and did not cause T cell activation or increased levels of proinflammatory cytokines in the sera.

319 The vectors established protection against a broad range of SARS-CoV-2 variants including the

320 recent Omicron subvariants BA.2.75, BA.4/5 and BQ.1. Protection was strongest against virus

321 with the parental D614G spike protein and somewhat less effective against the BA.2 variant, an

322 effect that was probably due to the relative decrease in spike protein affinity for ACE2[16].

323

324 Administration of the decoy-expressing AAV2.retro and AAV6.2 vectors by i.n. instillation

325 suppressed virus replication in the mice for at least 30 days. The effectiveness of i.n.

326 administration of the AAV2.retro vector, which was somewhat greater than the AAV6.2 vector,

327 was surprising as its capsid was selected for high efficiency transduction of the CNS and

328 retrograde transport in neurons[34,35]; its tropism for the respiratory tract has not, to our knowledge,

329 been previously described. The tropism of the AAV2.retro vector for lung and neuronal cells could

330 be clinically advantageous as a means to suppress SARS-CoV-2 replication in respiratory and

331 olfactory tissues. SARS-CoV-2 infection of ACE2 K18 Tg results in high virus loads in the brain

332 which was suppressed by administration of the decoy-expressing AAV2.retro vector (not shown).

333 Imaging of mice following administration of a luciferase-expressing AAV2.retro vector showed

334 transduction of the olfactory region of the brain (not shown).

335

336 In a previous report, Sims *et al*., used an AAV-expressed high affinity ACE2 decoy to protect mice

337 from SARS-CoV-2 infection[53]. In that study, i.n. administration of a decoy-expressing AAVhu.68

338 vector caused at 30-fold decrease in Wuhan-Hu-1 SARS-CoV-2 virus load 7-dpi but at 4-dpi,

339 close to the time at which virus loads peak, had no significant effect on virus loads. In contrast,

340 we found that i.n. or i.m. administration of decoy-expressing AAV2.retro or AAV6.2 vectors

341 decreased virus loads 10,000-100,000-fold at the time of peak virus load. The increased

342 effectiveness of the therapy in our study does not appear to have resulted from differences in

343 increased neutralizing activity of the decoys which appeared to be similar in both studies (IC50s

344 (37 ng/ml vs 20 ng/ml[29]) or differences in vector dosage which also appeared to be similar. A

345 potential explanation is that of more efficient transduction of respiratory tract cells by the

346 AAV2.retro and AAV6.2 vectors.

347

348   The effectiveness of i.m. injection with the AAV2.retro vector was encouraging because clinically

349   this route of administration may be more practical than i.n. instillation[43]. For reasons that are

350   unclear, i.m. injection of the AAV2.retro vector was 3-logs more effective than injection by that

351   route with the AAV6.2 vector. It is possible that the increased effectiveness of the vector was the

352   result of retrograde transport of the AAV2.retro capsid in myocytes or simply caused by more

353   efficient transduction of lung cells. The efficacy of i.m. injection of the vector suggests that decoy

354   protein synthesized by transduced myocytes at the site of injection diffuses systemically,

355   establishing a concentration in the respiratory tract sufficient to inhibit virus replication. Similarly,

356   in the rhesus macaque SIV model, i.m. administration of AAV vectors expressing broadly

357   neutralizing antibodies suppressed virus loads of SIV, a virus that replicates in secondary

358   lymphoid organs[3,39]. The long-lasting suppression of SIV replication by the vector suggests that

359   transduced terminally differentiated myocytes can produce AAV vector-encoded proteins for a

360   period of several years. Similarly, i.m. administration of a decoy-expressing AAV vector could

361   provide long-lived protection in humans. The protection could be more durable than that of the

362   extended half-life monoclonal antibodies currently in clinical use[44].

363

364   Unexpectedly, the decoy-expressing AAVs were also effective therapeutically. I.n. instillation of

365   the vectors as late as 24 hours post-SARS-CoV-2 infection suppressed virus replication, a time

366   course similar to what is found in the treatment of mice with highly potent neutralizing monoclonal

367   antibody[8]. The effectiveness of the decoy therapeutically demonstrates the rapid kinetics with

368   which the vectors transduce cells in the lung and program biosynthesis of the encoded protein. In

369   clinical practice, monoclonal antibody therapy is effective when given several days post-

370   infection[45]. The similarity in the timing with which the AAV vectors and monoclonal antibodies can

371   treat mice suggests that in humans, decoy-expressing AAV might be effective up to several days

17

372   post-infection, as is the case for the use of monoclonal antibodies. In mouse and hamster models,

373   the administration of recombinant ACE2 decoy protein has previously been shown to be highly

374   effective therapeutically[28,46]. The proteins do not require viral transduction or biosynthesis in the

375   lung and thus are expected to act faster; however, in clinical practice, their use will require large

376   quantities of highly pure recombinant protein which is not the case for vectored

377   immunoprophylaxis.

378

379   Delivery of the decoy protein with a lentiviral vector was also highly effective for the establishment

380   of vectored immunoprophylaxis. Like the AAV vectors, the lentiviral vector was most effective

381   administered by i.n. instillation, Unlike the AAV vectors, the lentiviral vector was also effective by

382   i.v. injection, a route that results mainly in the transduction of splenocytes, many of which are

383   DCs[47]. Lentiviral vectored immunoprophylaxis appeared to be more durable than AAV vector,

384   remaining fully intact through the 60-day time course. Interestingly, the level of virus load

385   suppression intensified at the later time points, an effect that was probably the result of increased

386   expression levels of the decoy in the in lung as demonstrated using a luciferase-expressing

387   reporter vector. The parameters that affected the durability of protection by the two types of

388   vectors are unclear. The AAV vectors transduced a significantly higher proportion of lung

389   endothelial cells while the lentiviral vector high transduced a high proportion of leukocytes, many

390   of which were DCs. Endothelial cells are mitotically active, thus diluting the AAV genome copy

391   number over time. DCs are terminally differentiated and could remain resident in the lung for a

392   long time.

393

394   AAV vectors are advantageous for clinical use because they are expressed long-term without

395   integrating into the host cell genome and are replication-defective[40,48-50]. The vectors are currently

396   in use in a large number of clinical trials for a broad range of diseases. There are over 20 AAV

397   serotypes, each with unique tissue tropism[51]. AAV6.2 is a variant of AAV6 that contains a single

398   point mutation (F129L) introduced to increase lung cell tropism[36]. AAV2.retro is an AAV2 variant

399   selected for retrograde transport in the CNS[52]. Both vectors administered i.n. protected mice from

400   infection. AAV2.retro, which has not been reported to transduce cells of the respiratory system

401   was, unexpectedly, somewhat more effective than AAV6.2. The majority of cells transduced by

402   both vectors were lung the epithelial cells although AAV2.retro transduced a large proportion of

403   neutrophils and monocytes.

404

405   The decoy-expressing lentiviral vector also strong protected mice from infection. Lentiviral vectors

406   are currently being developed for several clinical applications including CAR-T cells and SARS-

407   CoV-2 vaccines[54,55]. The vectors offer long-term expression and are not generally subject to pre-

408   existing immunity[56]. The protection established by i.n. administration of the decoy-expressing

409   vector remained intact over the 60-day time-course and was somewhat longer-lasting than that

410   of AAV vectored protection which started to wane after 30-days. The suppression of virus

411   replication by the lentiviral vector increased somewhat towards the end of the time-course, an

412   effect that was associated with a small increase in expression of the decoy-expressing lentiviral

413   vector in the lung. The increased durability of lentiviral-vectored immunoprophylaxis is

414   presumably the result of the transduction of a long-lived cell subpopulation in the lung although

415   the identity of this subpopulation is unclear. The lentiviral vector mainly transduced lung

416   leukocytes, many of which were DCs and monocytes that are thought to have short 2 day half-

417   lives[57,58] and thus unlikely to account for the durable expression. The AAV vectors transduced a

418   higher proportion of lung epithelial cells, a cell-type which in mice, has a much longer 17 month

419   half-life[59]. Possible explanations for the long-lasting protection provided by the lentiviral vector are

19

420   that a long-lived, subpopulation of tissue resident DC or myeloid cells had been transduced or

421   that integration of the vector allows for persistence of its genome in dividing cell subpopulations

422   of the lung. In most clinical applications, lentiviral vectors are used to transduce cells *ex vivo* that

423   are later re-infused, a procedure that has been generally viewed as low-risk. The safety profile of

424   integrating lentiviral vectors for direct injection has not been fully established[60-62].

425

426   A potential application of vectored immunoprophylaxis for SARS-CoV-2 is as a means of providing

427   protection to immunocompromised individuals for whom vaccination is less effective. Until

428   recently, the most effective protection available for such individuals was the AstraZeneca

429   Evusheld cocktail, a mixture of two monoclonal antibodies formulated for slow release by

430   intramuscular injection[44]. However, the therapy may have become less effective as a result of

431   immunoevasion by new Omicron subvariants. Both of the monoclonal antibodies in the cocktail

432   have decreased neutralizing titers against the Omicrons BA.1 and BA.2[5-14] and recent findings

433   suggest that they may be inactive against the increasingly prevalent BQ.1 and BA.2.75

434   subvariants[63]. This decrease in neutralizing activity contrasts with the decoy which maintains its

435   effectiveness against BQ.1 and BA.2.75.

436

437   AAV-based vectored immunoprophylaxis was effective therapeutically in the mouse models when

438   delivered within a 24-hour window post-infection. The short window is at least partially a function

439   of the rapid kinetics of virus replication and clearance in the mouse model as compared to in

440   humans. While the decoy-expressing AAV lost efficacy at later time points in the infected mouse,

441   the loss of effect was coincident with that found for treatment with a highly potent therapeutic

442   monoclonal antibody. Monoclonal antibody therapy has been found to lessen disease symptoms

443   when given to patients several days post-infection[45]. If the comparison pertains in humans, the

444   window for which the AAV therapy remains effective in humans might be comparable to that for

445   monoclonal antibody therapy.

446

447   Vectored immunoprophylaxis could be valuable in the case of a future pandemic spurred by the

448   zoonosis of a novel coronavirus. Species such as bats and pangolins harbor large numbers of

449   coronaviruses with the ability to use hACE2[64,65]. In the case of zoonosis of a coronavirus that used

450   ACE2 as its entry receptor, the decoy-expressing vectors reported here would be ready as an off-

451   the-shelf agent available prior to the production of a vaccine. The protection established by the

452   vectors is more rapid than of vaccine as it does not require the induction of an immune response.

453   In the case of zoonosis of a virus that used a receptor other than ACE2 or if a novel SARS-CoV-

454   2 variant were to emerge that switched its receptor usage, the decoy receptor approach could

455   also be applicable. This would involve the identification of the entry receptor for the novel virus

456   and the construction of a soluble form of the protein to serve as a decoy. While a switch in receptor

457   usage is possible, it has not happened to date despite strong selective pressure on the viral spike

458   protein to alter its amino acid sequence.

459 **STAR Methods**

460 **Resource Availability**

461 **Lead Contact**

462 Further information and requests for resources and reagents should be directed to and will be

463 fulfilled by the Lead Contact, Nathaniel R. Landau (nathaniel.landau@med.nyu.edu).

464

465 **Materials Availability**

466 All unique DNA constructs, proteins and pseudotyped virus generated in this study are available

467 from the Lead Contact upon request.

468

469 **Data and Code Availability**

470 • The data used in this study are available upon request from the lead contact.

471 • This paper does not report original code.

472 • Any additional information required to reanalyze the data reported in this paper is

473 available from the lead contact upon request.

474

475 **Experimental Model and Subject Details**

476

477 **Cells**

478 293T cells were cultured in DMEM/10% FBS. Clonal cell-lines CHME3.ACE2 and A549.ACE2

479 were established by lipofection of CHME3 and A549 cells with plenti.ACE2[6] using

480 lipofectamine2000 (Invitrogen). The cells were selected in 1 μg/ml puromycin and single cell

481 clones were evaluated by flow cytometry for high ACE2 expression. CHME3.ACE2, A549.ACE2

482 and ACE2.TMPRSS2.Vero E6 cells were maintained in medium with 1 μg/ml puromycin. hSABCi-

483   NS1.1 cells were differentiated in air-liquid interface cultures in transwell dishes at 1.5×10^5

484   cells/well. The cells were plated onto inserts coated with human type IV collagen (Sigma) in

485   PneumaCult Ex Plus medium (Stemcell Technologies). The cells were cultured at 37 °C under

486   5% CO_2. The medium in the upper and lower chambers was changed one day after plating and

487   the medium in the lower chamber was replaced every 2 days. The medium in the upper chamber

488   was removed the apical surface was washed with PBS weekly for 2 weeks.

489

490   **Mice**

491   C57BL/6 mice were from Taconic. Balb/c and hACE2 K18 Tg [B6.Cg-Tg(K18-ACE2)2Prlmn/J]

492   were from The Jackson Laboratory. Animal use and care was approved by the NYU Langone

493   Health Institutional Animal Care and Use Committee (#170304) according to the standards set by

494   the Animal Welfare Act.

495

496   **Plasmids**

497   The expression vectors used for the production of AAV vectors were AAV.retro Rep/Cap2

498   (Addgene 81070), Rep/Cap6 (Addgene 110770), pAdDeltaF6 (Addgene 112867) and pAAV-

499   CAG-tdTomato. Rep/Cap6.2 expression plasmid was generated by overlap extension PCR using

500   Rep/Cap6 template to introduce the F129L mutation. The amplicon was cloned into the EcoR-I

501   and Nru-I sites of Rep/Cap6. To construct GFP/nanoluciferase-expressing AAV vectors pAAV-

502   GFP.nLuc, pAAV-CAG-ACE2.1mb.nLuc and pAAV-CAG-ACE2.1mb, DNA fragments encoding

503   GFP.nLuc, ACE2.1mb.nLuc and ACE2.1mb were amplified by PCR and joined by overlap

504   extension PCR using primers containing Kpn-I and EcoR-I sites. The insert was removed from

505   pAAV-CAG-tdTomato by cleavage with Kpn-I and EcoR-I and replaced with similarly cleaved

506   amplicon. Decoy expression vector pcACE2.1mb has been previously described[21]. Expression

507   plasmids used to produce lentiviral pseudotypes were pMDL, pcVSV.G, pRSV.Rev, the lentiviral

508   transfer vector plenti.GFP.nLuc[6]. Expression vectors for the SARS-CoV-2 D614G, Omicron BA.1,

509   Omicron BA.2 spike proteins have been previously described[9,12,21]. Expression vectors for the

510   Omicron BA.4/5, BA.2.75 and BQ.1 spike proteins were constructed by overlap extension PCR

511   mutagenesis using the D614G[5] spike protein plasmid as template and cloned into pcDNA6.

512

513   **Method Details**

514

515   **AAV vector stocks**

516   AAV vector stocks were produced by cotransfection of 293T cells with pAAV-CAG-ACE2.1mb,

517   pAdDeltaF6 and AAV.retro RepCap2 or Rep/Cap6.2 at a ratio of 25:25:30 by the calcium

518   phosphate method. Virus-containing supernatant was harvested 2 days post-transfection. The

519   virus was concentrated by ultracentrifugation on 40% sucrose cushion at 4°C for 16 hours at

520   30,000 x g, resuspended in PBS and concentrated on an Amicon Ultra Centrifugal Filter Unit

521   (Millipore). Virus titers were measured by RT-qPCR with a primer pair and probe that hybridized

522   to the AAV2 ITR sequences[66].

523

524   **SARS-CoV-2 virus stocks**

525   SARS-CoV-2 WA1/2020 (BEI Resources, NR-52281), Omicron BA.1 (BEI Resources, NR-

526   56461), BA.2 (BEI Resources, NR-56781) and BA.5 virus (BEI Resources, NR-58616) stocks

527   were prepared by infection of ACE2.TMPRSS2.Vero E6 cells at an MOI=0.05 (BEI Resources,

528   NR-56781). 2 hours post-infection, the input virus was removed and a day later, the virus-

529   containing supernatant was filtered through a 0.45 μm filter, concentrated on an Amicon Ultra

530   Centrifugal Filter Unit (Millipore) and frozen at -80°C in aliquots.

24

531

Decoy pull-down

533   CHME3.ACE2 or A549.ACE2 cells (1 x 10^6) were infected with AAV2.retro, AAV6.2-ACE2.1mb

534   or plenti.ACE2.1mb at MOI=0.5. The virus was removed the following day and the supernatant

535   was harvested 3 days later. The decoy protein was pulled-down by a 1-hour incubation with 30 μl

536   nickel-nitrilotriacetic acid-agarose beads (QIAGEN) and eluted in Laemmle loading buffer. The

537   protein was then analyzed on an immunoblot probed with anti-His antibody and horseradish

538   peroxidase (HRP)-conjugated goat anti-mouse IgG secondary antibody (Sigma-Aldrich). The

539   signals were developed with Immobilon Crescendo Western HRP Substrate (Millipore) and

540   visualized on an iBright imaging system (Invitrogen).

541

Pseudotype neutralization assay

543   D614G, BA.1, BA.2, BA.2.75, BA.4/5 and BQ.1 spike protein-pseudotyped lentiviruses were

544   generated by co-transfection of 293T cells with pMDL, pRSV.Rev, plenti.GFP.nLuc and spike

545   protein expression vector and normalized for reverse transcriptase activity as previously

546   described[5]. CHME3.ACE2 and A549.ACE2 cells were transduced with serially diluted decoy-

547   expressing AAV or lentiviral vector. The medium was removed the following day and the cells

548   were challenged with pseudotyped viruses (MOI=0.2). Luciferase activity in duplicate samples

549   was measured 2-dpi in an Envision 2103 microplate luminometer (PerkinElmer).

550

Flow cytometry

552   GFP-expressing AAV or lentiviral vectors were injected into hACE2 K18 Tg (AAV) or SAMHD1

553   Knockout mice (lentivirus) via i.n. injection. At 3-dpi, the lungs were homogenized in ACK buffer

554   and the cells were disaggregated by a 30-minute treatment with 1.5 mg/mL collagenase and 0.1

555 mg/mL DNase followed by passage through a 0.22 μm mesh. The cells were blocked with anti-

556 CD16/CD32 and stained with Alexa 700-anti-CD45, PerCP-Cy5.5-anti-F4/80, APC-Cy7-SiglecF,

557 PE-Cy7-anti-CD11c, PE-Cy7-anti-CD19, APC-anti-CD3, Pacblue-anti-CD11b, PE-Cy5.5-anti-

558 CD62L, APC-anti-CD14 and PE-Ly6C/Ly6G (Gr1) (BioLegend) and analyzed on a Beckman

559 CytoFLEX flow cytometer using with FlowJo software. Cell-types were classified as epithelial

560 (CD45-), alveolar macrophages (CD45+, F4/80+, SiglecF+), interstitial macrophages (CD45+,

561 F4/80+, SiglecF-), DCs (CD45+, F4/80-, CD11c+), T cells (CD45+, CD3+), B cells (CD45+,

562 CD19+), monocytes (CD45+, CD11b+, CD14+) and neutrophils (CD45+, CD62L+, Ly6C/Ly6G+).

563

564 **Anti-inflammatory cytokine assay**

565 hACE2 K18 Tg were administrated 1×10^{12} vg decoy-expressing AAV or 5×10^6 IU decoy-

566 expressing lentiviral vector. Mice treated with AAV or lentiviral vector were challenged 3- or 7-

567 days later, respectively, with 2×10^4 PFU SARS-CoV-2 WA1/2020. Sera were harvested 3-dpi

568 and IFN-γ, MCP-1, TNF-α, IL-10, IL-12 and IL-6 were measured by cytokine bead array using the

569 BD Cytometric Bead Array Mouse Inflammation Kit (BD Biosciences).

570

571 *In vivo* and *in vitro* **luciferase assays**

572 Balb/c or SAMHD1 knockout mice were administered AAV2.retro or AAV6.2-ACE2.1mb.nLuc (1×

573 10^{12} vg) or plenti.GFP.nLuc (5×10^6 IU) by i.n. instillation. The mice were imaged over 30 days by

574 the injection of 100 μl 1:40 diluted Nano-Glo substrate (Nanolight) and visualization on an IVIS

575 Lumina III XR (PerkinElmer). To measure luciferase activity in the tissues, organs were harvested

576 and homogenized in lysing matrix D tubes with a FastPrep-24 5G homogenizer (MP Biomedicals).

577 Nano-Glo Luciferase Assay Reagent (Nanolight) was added and luminescence was measured on

578 an Envision 2103 plate reader (PerkinElmer).

26

579

Live virus infection of cell-lines

CHME3.ACE2, A549.ACE2 and hSABCi-NS1.1 cells (2×10^5) were infected with AAV2.retro or

AAV6.2-ACE2.1mb at MOI=0.5. The medium was replaced 1-dpi and the following day, the cells

were infected with SARS-CoV-2 at MOI=0.01. The cultures were lysed 2-dpi after which RNA was

prepared and cell-associated viral RNA copies were quantified by reverse transcriptase RT-qPCR.

Absolute RNA copy numbers were calculated using a standard curve generated by the analysis

of a serially diluted *in vitro* transcribed synthetic subgenomic viral RNA using the 2−ΔΔCT method.

587

Prophylactic and therapeutic administration of decoy-expressing vectors.

For prophylaxis experiment, 6-8 weeks old hACE2 K18 Tg or Balb/c mice were anesthetized with

isoflurane or ketamine–xylazine cocktail and injected with 80 μl (i.n. or i.v. or i.m.) (1×10^{12} vg) of

AAV2.retro or AAV6.2-decoy or 5×10^6 IU of plenti.ACE2.1mb. After 1-30 days (AAV) and 1-60

days (lentivirus vector) of infection, the mice were infected i.n. with 2×10^4 plaque-forming unit

(PFU) of SARS-CoV-2 WA1/2020 (hACE2 K18 Tg) or Omicron BA.1 or BA.2 or BA.5 (Balb/c). At

2-dpi (Omicron) or 3-dpi (SARS-CoV-2 WA1/2020), the mice were sacrificed and RNA was

prepared from 200 μl of lung lysate using the Quick-RNA MiniPrep kit (Zymo Research). For

therapeutic testing, hACE2 K18 Tg were infected i.n. with 2×10^4 PFU SARS-CoV-2 WA1/2020.

The mice were infected 0-48 hours post-infection i.n. with 80 μl (1×10^{12} vg) of AAV2.retro or

AAV6.2-decoy. 3-dpi (SARS-CoV-2 WA1/2020), the mice were sacrificed and RNA was prepared

from 200 μl of the lung lysate using a Quick-RNA MiniPrep kit.

600

Virus loads

27

602　SARS-CoV-2 E gene subgenomic RNA levels were measured by reverse transcriptase RT-qPCR

603　with a TaqMan probe. Lung RNA was mixed with TaqMan Fast Virus 1-step Master Mix (Applied

604　Biosystems), 10 mM forward and reverse primers, and 2 mM probe. PCR cycles were 5 minutes

605　at 50°C, 20 seconds at 95°C, 40 cycles of 3 seconds at 95°C, 3 seconds at 60°C). E gene

606　subgenomic RNA copies were measured using forward primer subgenomic F

607　(CGATCTCTTGTAGATCTGTTCTC), reverse primer E Sarbeco R and probe E Sarbeco P1)[67,68].

608　Tissue analyses were normalized to GAPDH mRNA copies measured using the mouse

609　GAPDH.forward (CAATGTGTCCGTCGTGGATCT) and mouse GAPDH.reverse

610　(GTCCTCAGTGTAGCCCAAGATG) with mouse GAPDH probe (FAM-

611　CGTGCCGCCTGGAGAAACCTGCC-BHQ) or human GAPDH.forward

612　(GTCTCCTCTGACTTCAACAGCG) and human GAPDH.reverse

613　(ACCACCCTGTTGCTGTAGCCAA) with human GAPDH probe (FAM-TAGGAAGGACAGGCAAC-

614　IBFQ). Absolute RNA copy numbers were calculated using a standard curve generated by the

615　analysis of a serially diluted *in vitro* transcribed synthetic subgenomic viral RNA containing the E

616　gene sequence (2019-nCoV_E Positive Control, IDT: 10006896) using the $2^{-\Delta\Delta CT}$ method.

617

618　**Histology**

619　The lungs of SARS-CoV-2-infected mice were harvested 3-dpi. The tissue was fixed in 10%

620　neutral buffered formalin for 72 hours at room temperature and then processed through graded

621　ethanol, xylene and into paraffin in a Leica Peloris automated processor. 5 μm paraffin-embedded

622　sections were deparaffinized and stained with hematoxylin (Leica, 3801575) and eosin (Leica,

623　3801619) on a Leica ST5020 automated histochemical strainer. Slides were scanned at 40×

624　magnification on a Leica AT2 whole slide scanner and the images were transferred to the NYULH

625　Omero web-accessible image database.

28

626

Statistical Analysis

Statistical significance was determined by Kruskal-Wallis test with post hoc Dunn's test. Significance was calculated based on two-sided testing and is shown in the figures as the mean ± SD with confidence intervals listed as $*p<0.05$, $**p<0.01$, $***p<0.001$, $****p<0.0001$.

631

Study Approval

Animal procedures were performed with the written approval of the NYU Animal Research Committee in accordance with all federal, state, and local guidelines.

635

640

645

Author Contributions

T.T. and N.R.L. designed the experiments. T.T., B.M.D. and J.M. carried out the experiments. T.T. and N.R.L. wrote the manuscript. N.R.L. supervised the study and revised the manuscript.

649   **Figure legends**

650

651   **Figure 1. AAV-ACE2.1mb prevents SARS-CoV-2 infection in cell culture.**

652   (A) The domain structure of full-length ACE2 is shown above with the ectodomain,

653   transmembrane (TM) and intracellular domain (IC). The structure of the decoy consisting of the

654   ACE2 ectodomain, human IgG1-CH3 and carboxy-terminal His tag. The ACE2 domain contains

655   three high affinity mutations as described by Chan et al. and a H345A mutation in the ACE2

656   peptidase catalytic site.

657   (B) A549.ACE2 and CHME3.ACE2 cells were transduced with a 5-fold serial dilution of

658   AAV2.retro and AAV6.2 decoy vectors and then challenged with ancestral D614G, Omicron BA.1,

659   BA.2, BA.2.75, BA.4/5 and BQ1 spike protein-pseudotyped lentiviral vectors. Luciferase activity

660   was measured 2-dpi. The curves shown above indicate the infectivity based on luciferase activity

661   normalized to mock vector-transduced cells. Each measurement is shown as the average of

662   duplicates. The table below shows that ID_{50} calculated from the curves shown above.

663   (C) CHME3.ACE2 and A549.ACE2 cells were transduced with AAV2.retro-GFP.nLuc (GFP.Luc),

664   AAV6.2-GFP.nLuc, AAV2.retro-ACE2.1mb, AAV6.2-ACE2.1mb at MOI=0.5. 2 days post

665   transduction, the cells were infected with SARS-CoV-2 WA1/2020 (MOI=0.01). The cultures were

666   lysed 2-dpi and RNA was prepared. Viral RNA copy numbers were determined by RT-qPCR.

667   (D) hSABCi-NS1.1 cells were transduced with AAV2.retro-GFP.nLuc, AAV6.2-GFP.nLuc,

668   AAV2.retro-ACE2.1mb, AAV6.2-ACE2.1mb at MOI=0.5. 2 days post transduction, the cells were

669   infected with SARS-CoV-2 WA1/2020 (MOI=0.01). The cultures were lysed 2-dpi and RNA was

670   prepared. Viral RNA copy numbers were determined by RT-qPCR. Confidence intervals are

671   shown as the mean ± SD. **P ≤ 0.01. The experiment was done twice with similar results.

672   (E) CHME3.ACE2 and A549.ACE2 cells were transduced with AAV2.retro or AAV6.2-ACE2.1mb

673   at MOI=0.5. 3-dpi, secreted decoy protein in the supernatant was pulled-down on NTA beads and

674   bead-bound decoy was detected on an immunoblot probed with His-tag antibody. Pure

675   recombinant decoy protein is shown at right as a standard and was used to determine the amount

676   of protein pulled-down, which is shown below each lane as micrograms decoy pulled-down from

677   1 ml of culture supernatant. At right is shown decoy protein in the cell lysates is shown below with

678   GAPDH as a loading control.

679

680   **Figure 2. Vectored immunoprophylaxis by decoy-expressing AAV decoy vector and**

681   **therapeutic use**.

682   (A) The experimental scheme for testing decoy prophylaxis is diagrammed. hACE2 K18 Tg and

683   Balb/c mice were treated by i.v. injection or i.n. instillation with decoy-expressing AAV vector or

684   control GFP.nLuc-expressing AAV vector (1 X 10^{12} vg). 3 days post-treatment, the hACE2 K18

685   Tg mice were challenged with SARS-CoV-2 WA1/2020 and the Balb/c mice were challenged with

686   Omicron BA.1, BA.2 or BA.5 (2 x 10^4 PFU). Viral RNA copies were quantified 2 days (Omicron)

687   or 3 days (SARS-CoV-2 WA1/2020) post-infection.

688   (B) Mice (n=3-4) were treated with decoy-expressing or control GFP-expressing AAV vectors and

689   challenged with SARS-CoV-2 WA1/2020. Viral RNA copies in the lungs were quantified 3-dpi.

690   (C) H&E stained lung sections from control and decoy-expressing AAV vectors and SARS-CoV-

691   2 infected mice are shown on the left (2 x, scale bars 500µm) and with the boxed area enlarged

692   on the right **(**20 x, scale bars 50µm**)**.

693   (D) Mice (n=3) were treated with decoy-expressing AAV vectors on day 0 and challenged with

694   SARS-CoV-2 WA1/2020 on day 3. Body weight was measured daily. As controls, the mice were

695   infected with SARS-CoV-2 WA1/2020 but not treated with AAV vector or treated with AAV vector

696   but not infected with SARS-CoV-2 WA1/2020.

697   (E) Balb/c mice (n=3-4) were treated with decoy-expressing or GFP-expressing control AAV

698   vectors and then infected 3 days later with Omicron BA.1, BA.2, or BA.5. Viral RNA copies in the

699   lungs were quantified 2-dpi.

700   (F) Mice (n=4) were administered decoy-expressing AAV vectors i.m. or i.v. and challenged 3-dpi

701   with SARS-CoV-2 WA1/2020. Infected but untreated and uninfected/untreated mice are included

702   as controls.

703   G. Therapeutic use of the decoy-expressing AAV vectors was tested as diagrammed (left). hACE2

704   K18 Tg (n=4) were infected with SARS-CoV-2 WA1/2020 (2×10^4 PFU) and then treated with

705   decoy-expressing AAVs at time-points up to 48 hours post-infection. Viral RNA in the lung was

706   quantified 3-dpi (right). As controls the mice were untreated (No AAV) or uninfected. Confidence

707   intervals are shown as the mean ± SD. ***$P \leq 0.001$, ****$P \leq 0.0001$. The experiment was done twice

708   with similar results.

709

710   **Figure 3. Durable vectored immunoprophylaxis by decoy-expressing AAV vectors.**

711   (A) Balb/c mice (n=3) were injected i.n. with decoy-luciferase fusion protein-expressing AAV

712   vectors (1×10^{12} vg). Luciferase activity was visualized by live imaging over 30 days at the

713   indicated time points. Representative images of a mouse from each group are shown.

714   (B) Luciferase activity in lung tissue homogenates from mice treated with the decoy-luciferase

715   expressing AAV vectors (n=2) was measured over the time course.

716   (C) The experimental scheme to test the durability of AAV vectored immunoprophylaxis is

717   diagrammed (left). hACE2 K18 Tg (n=4) were injected with AAV decoy. At 1-, 2-, 3-dpi, the mice

718   were challenged with SARS-CoV-2 (2×10^4 PFU) and viral RNA in the lungs was quantified. The

32

719   results are shown as a histogram (right). SARS-CoV-2 infected/AAV untreated (No AAV) and AAV

720   untreated/SARS-CoV-2 uninfected (Uninfected) controls are shown. Confidence intervals are

721   shown as the mean ± SD. ****$P \leq 0.0001$. The experiment was done twice with similar results.

722

723   **Figure 4. Long-term vectored immunoprophylaxis by decoy-expressing lentiviral vector.**

724   (A) A549.ACE2 and CHME3.ACE2 cells were transduced with a 5-fold serial dilution of decoy-

725   expressing lentiviral vectors and then challenged with D614G, Omicron BA.1, BA.2, 2.75, BA.4/5

726   and BQ.1 spike protein-pseudotyped lentiviral vectors. Luciferase activity was measured 2-dpi

727   (above). The curves indicate infectivity based on luciferase activity normalized to mock vector-

728   transduced cells. Measurements are the average of duplicates. ID_{50}s calculated from the curves

729   are shown in the table (below).

730   (B) Structure of lentiviral vector and experimental scheme are shown. hACE2 K18 Tg mice or

731   Balb/c were injected with lentiviral vector (5×10^6 IU) i.p., i.v. or i.n. injection. One week later, the

732   mice were challenged with 2×10^4 PFU of SARS-CoV-2 WA1/2020 (hACE2 K18 Tg) or Omicron

733   (Omicron). Viral RNA in the lungs was quantified 3-dpi.

734   (C) Mice were administered luciferase-expressing lentiviral vector i.v. or i.n. (n=2). Tissues (nasal,

735   lung, trachea, spleen and liver) were harvested and luciferase activity was measured over 60

736   days at the indicated time-points.

737   (D) Decoy-expressing lentiviral vectors (5×10^6 IU) were administered i.v. or i.n. and after 7-, 30-

738   and 60-days challenged with SARS-CoV-2 (2×10^4 PFU). Viral RNA was quantified 3-dpi.

739   Confidence intervals are shown as the mean ± SD. **$P \leq 0.01$, ****$P \leq 0.0001$. The experiment was

740   done twice with similar results.

741

742   **Figure 5. Comparison of lung cell subpopulations transduced by AAV and lentiviral vectors.**

743   (A) GFP-expressing AAV vectors were administrated i.n. After 3 days, the lungs were harvested

744   and the tissue were enzymatically disaggregated. The cells were analyzed by multi-color flow

745   cytometry with cell-type specific marker antibodies to distinguish subpopulations defined as

746   follows: Leukocytes (CD45+), epithelial (CD45-), alveolar macrophages (CD45+, F4/80+,

747   SiglecF+), interstitial macrophages (CD45+, F4/80+, SiglecF-), DCs (CD45+, F4/80-, CD11c+), T

748   cells (CD45+, CD3+), B cells (CD45+, CD19+), monocytes (CD45+, CD11b+, CD14+),

749   neutrophils (CD45+, CD62L+, Ly6C/Ly6G+). Representative flow cytometry plots of the GFP+

750   cells and GFP+/CD45+ populations are shown on the left and the subpopulations within the

751   GFP+/CD45+ leukocytes are shown in the pie charts on the right.

752   (B) Mice were administered GFP-expressing lentiviral vector i.n. GFP+ cells in the lung were

753   analyzed by flow cytometry as in (A). Representative flow cytometry plots of the GFP+ cells and

754   GFP+/CD45+ populations are shown on the left and the subpopulations within the GFP+/CD45+

755   leukocytes are shown in the pie charts on the right.

References

756

757   1.   Johnson, P.R., Schnepp, B.C., Zhang, J., Connell, M.J., Greene, S.M., Yuste, E.,

758   Desrosiers, R.C., and Clark, K.R. (2009). Vector-mediated gene transfer engenders

759   long-lived neutralizing activity and protection against SIV infection in monkeys. Nat Med

760   *15*, 901-906. 10.1038/nm.1967.

761   2.   Gardner, M.R. (2020). Promise and Progress of an HIV-1 Cure by Adeno-Associated

762   Virus Vector Delivery of Anti-HIV-1 Biologics. Front Cell Infect Microbiol *10*, 176.

763   10.3389/fcimb.2020.00176.

764   3.   Gardner, M.R., Kattenhorn, L.M., Kondur, H.R., von Schaewen, M., Dorfman, T., Chiang,

765   J.J., Haworth, K.G., Decker, J.M., Alpert, M.D., Bailey, C.C., et al. (2015). AAV-

766   expressed eCD4-Ig provides durable protection from multiple SHIV challenges. Nature

767   *519*, 87-91. 10.1038/nature14264.

768   4.   Taylor, P.C., Adams, A.C., Hufford, M.M., de la Torre, I., Winthrop, K., and Gottlieb, R.L.

769   (2021). Neutralizing monoclonal antibodies for treatment of COVID-19. Nat Rev Immunol

770   *21*, 382-393. 10.1038/s41577-021-00542-x.

771   5.   VanBlargan, L.A., Errico, J.M., Halfmann, P.J., Zost, S.J., Crowe, J.E., Jr., Purcell, L.A.,

772   Kawaoka, Y., Corti, D., Fremont, D.H., and Diamond, M.S. (2022). An infectious SARS-

773   CoV-2 B.1.1.529 Omicron virus escapes neutralization by therapeutic monoclonal

774   antibodies. Nat Med. 10.1038/s41591-021-01678-y.

775   6.   Liu, L., Iketani, S., Guo, Y., Chan, J.F.W., Wang, M., Liu, L., Luo, Y., Chu, H., Huang, Y.,

776   Nair, M.S., et al. (2022). Striking antibody evasion manifested by the Omicron variant of

777   SARS-CoV-2. Nature *602*, 676-681. 10.1038/s41586-021-04388-0.

778   7.   Planas, D., Saunders, N., Maes, P., Guivel-Benhassine, F., Planchais, C., Buchrieser,

779   J., Bolland, W.-H., Porrot, F., Staropoli, I., Lemoine, F., et al. (2021). Considerable

780   escape of SARS-CoV-2 Omicron to antibody neutralization. Nature. 10.1038/s41586-

781   021-04389-z.

782 8. Dragoni, F., Schiaroli, E., Micheli, V., Fiaschi, L., Lai, A., Zehender, G., Rossetti, B.,

783   Gismondo, M.R., Francisci, D., Zazzi, M., and Vicenti, I. (2022). Impact of SARS-CoV-2

784   omicron BA.1 and delta AY.4.2 variants on the neutralization by sera of patients treated

785   with different authorized monoclonal antibodies. Clin Microbiol Infect.

786   10.1016/j.cmi.2022.03.005.

787 9. Zhou, H., Dcosta, B.M., Landau, N.R., and Tada, T. (2022). Resistance of SARS-CoV-2

788   Omicron BA.1 and BA.2 Variants to Vaccine-Elicited Sera and Therapeutic Monoclonal

789   Antibodies. Viruses *14*. 10.3390/v14061334.

790 10. Iketani, S., Liu, L., Guo, Y., Liu, L., Chan, J.F.W., Huang, Y., Wang, M., Luo, Y., Yu, J.,

791   Chu, H., et al. (2022). Antibody evasion properties of SARS-CoV-2 Omicron

792   sublineages. Nature *604*, 553-556. 10.1038/s41586-022-04594-4.

793 11. Chen, R.E., Winkler, E.S., Case, J.B., Aziati, I.D., Bricker, T.L., Joshi, A., Darling, T.L.,

794   Ying, B., Errico, J.M., Shrihari, S., et al. (2021). In vivo monoclonal antibody efficacy

795   against SARS-CoV-2 variant strains. Nature *596*, 103-108. 10.1038/s41586-021-03720-

796   y.

797 12. Tada, T., Zhou, H., Dcosta, B.M., Samanovic, M.I., Chivukula, V., Herati, R.S., Hubbard,

798   S.R., Mulligan, M.J., and Landau, N.R. (2022). Increased resistance of SARS-CoV-2

799   Omicron variant to neutralization by vaccine-elicited and therapeutic antibodies.

800   EBioMedicine *78*, 103944. 10.1016/j.ebiom.2022.103944.

801 13. Diamond, M., Halfmann, P., Maemura, T., Iwatsuki-Horimoto, K., Iida, S., Kiso, M.,

802   Scheaffer, S., Darling, T., Joshi, A., Loeber, S., et al. (2021). The SARS-CoV-2

803   B.1.1.529 Omicron virus causes attenuated infection and disease in mice and hamsters.

804   Res Sq. 10.21203/rs.3.rs-1211792/v1.

805 14. Bruel, T., Hadjadj, J., Maes, P., Planas, D., Seve, A., Staropoli, I., Guivel-Benhassine,

806   F., Porrot, F., Bolland, W.H., Nguyen, Y., et al. (2022). Serum neutralization of SARS-

807   CoV-2 Omicron sublineages BA.1 and BA.2 in patients receiving monoclonal antibodies.

808   Nat Med. 10.1038/s41591-022-01792-5.

809 15. Touret, F., Baronti, C., Pastorino, B., Villarroel, P.M.S., Ninove, L., Nougairede, A., and

810   de Lamballerie, X. (2022). In vitro activity of therapeutic antibodies against SARS-CoV-2

811   Omicron BA.1, BA.2 and BA.5. Sci Rep *12*, 12609. 10.1038/s41598-022-16964-z.

812 16. Cao, Y., Yisimayi, A., Jian, F., Song, W., Xiao, T., Wang, L., Du, S., Wang, J., Li, Q.,

813   Chen, X., et al. (2022). BA.2.12.1, BA.4 and BA.5 escape antibodies elicited by Omicron

814   infection. Nature *608*, 593-602. 10.1038/s41586-022-04980-y.

815 17. Imai, M., Ito, M., Kiso, M., Yamayoshi, S., Uraki, R., Fukushi, S., Watanabe, S., Suzuki,

816   T., Maeda, K., Sakai-Tagawa, Y., et al. (2022). Efficacy of Antiviral Agents against

817   Omicron Subvariants BQ.1.1 and XBB. N Engl J Med. 10.1056/NEJMc2214302.

818 18. Czajkowsky, D.M., Hu, J., Shao, Z., and Pleass, R.J. (2012). Fc-fusion proteins: new

819   developments and future perspectives. EMBO Mol Med *4*, 1015-1028.

820   10.1002/emmm.201201379.

821 19. Hodges, T.L., Kahn, J.O., Kaplan, L.D., Groopman, J.E., Volberding, P.A., Amman, A.J.,

822   Arri, C.J., Bouvier, L.M., Mordenti, J., and Izu, A.E. (1991). Phase 1 study of

823   recombinant human CD4-immunoglobulin G therapy of patients with AIDS and AIDS-

824   related complex. Antimicrobial Agents and Chemotherapy *35*, 2580-2586.

825   doi:10.1128/AAC.35.12.2580.

826   20.   Gershon, D. (1996). Genentech sheds gp120 vaccine. Nature Medicine *2*, 370-371.

827   10.1038/nm0496-370.

828   21.   Tada, T., Fan, C., Chen, J.S., Kaur, R., Stapleford, K.A., Gristick, H., Dcosta, B.M.,

829   Wilen, C.B., Nimigean, C.M., and Landau, N.R. (2020). An ACE2 Microbody Containing

830   a Single Immunoglobulin Fc Domain Is a Potent Inhibitor of SARS-CoV-2. Cell Rep *33*,

831   108528. 10.1016/j.celrep.2020.108528.

832   22.   Chan, K.K., Dorosky, D., Sharma, P., Abbasi, S.A., Dye, J.M., Kranz, D.M., Herbert,

833   A.S., and Procko, E. (2020). Engineering human ACE2 to optimize binding to the spike

834   protein of SARS coronavirus 2. Science *369*, 1261-1265. 10.1126/science.abc0870.

835   23.   Jing, W., and Procko, E. (2021). ACE2-based decoy receptors for SARS coronavirus 2.

836   Proteins *89*, 1065-1078. 10.1002/prot.26140.

837   24.   Zhang, L., Narayanan, K.K., Cooper, L., Chan, K.K., Skeeters, S.S., Devlin, C.A.,

838   Aguhob, A., Shirley, K., Rong, L., Rehman, J., et al. (2022). An ACE2 decoy can be

839   administered by inhalation and potently targets omicron variants of SARS-CoV-2. EMBO

840   Molecular Medicine *14*, e16109. https://doi.org/10.15252/emmm.202216109.

841   25.   Linsky, T.W., Vergara, R., Codina, N., Nelson, J.W., Walker, M.J., Su, W., Barnes, C.O.,

842   Hsiang, T.Y., Esser-Nobis, K., Yu, K., et al. (2020). De novo design of potent and

843   resilient hACE2 decoys to neutralize SARS-CoV-2. Science *370*, 1208-1214.

844   10.1126/science.abe0075.

845   26.   Higuchi, Y., Suzuki, T., Arimori, T., Ikemura, N., Mihara, E., Kirita, Y., Ohgitani, E.,

846   Mazda, O., Motooka, D., Nakamura, S., et al. (2021). Engineered ACE2 receptor therapy

847   overcomes mutational escape of SARS-CoV-2. Nature Communications *12*, 3802.

848   10.1038/s41467-021-24013-y.

849   27.   Case, J.B., Rothlauf, P.W., Chen, R.E., Liu, Z., Zhao, H., Kim, A.S., Bloyet, L.M., Zeng,

850   Q., Tahan, S., Droit, L., et al. (2020). Neutralizing Antibody and Soluble ACE2 Inhibition

851   of a Replication-Competent VSV-SARS-CoV-2 and a Clinical Isolate of SARS-CoV-2.

852   Cell Host Microbe. 10.1016/j.chom.2020.06.021.

853   28.   Zhang, L., Dutta, S., Xiong, S., Chan, M., Chan, K.K., Fan, T.M., Bailey, K.L., Lindeblad,

854   M., Cooper, L.M., Rong, L., et al. (2022). Engineered ACE2 decoy mitigates lung injury

855   and death induced by SARS-CoV-2 variants. Nat Chem Biol *18*, 342-351.

856   10.1038/s41589-021-00965-6.

857   29.   Tada, T., Dcosta, B.M., Zhou, H., and Landau, N.R. (2023). ACE2 Receptor Decoy is a

858   Potent Prophylactic and Therapeutic for SARS-CoV-2. bioRxiv, 2022.2012.2031.522401.

859   10.1101/2022.12.31.522401.

860   30.   Guy, J.L., Jackson, R.M., Jensen, H.A., Hooper, N.M., and Turner, A.J. (2005).

861   Identification of critical active-site residues in angiotensin-converting enzyme-2 (ACE2)

862   by site-directed mutagenesis. FEBS J *272*, 3512-3520. 10.1111/j.1742-

863   4658.2005.04756.x.

864   31.   Meyer-Berg, H., Zhou Yang, L., Pilar de Lucas, M., Zambrano, A., Hyde, S.C., and Gill,

865   D.R. (2020). Identification of AAV serotypes for lung gene therapy in human embryonic

866   stem cell-derived lung organoids. Stem Cell Res Ther *11*, 448. 10.1186/s13287-020-

867   01950-x.

868   32.   van Lieshout, L.P., Domm, J.M., and Wootton, S.K. (2019). AAV-Mediated Gene

869   Delivery to the Lung. Methods Mol Biol *1950*, 361-372. 10.1007/978-1-4939-9139-6_21.

870   33.   Halbert, C.L., Allen, J.M., and Miller, A.D. (2001). Adeno-associated virus type 6 (AAV6)

871   vectors mediate efficient transduction of airway epithelial cells in mouse lungs compared

872   to that of AAV2 vectors. J Virol *75*, 6615-6624. 10.1128/JVI.75.14.6615-6624.2001.

873   34.   Tervo, D.G., Hwang, B.Y., Viswanathan, S., Gaj, T., Lavzin, M., Ritola, K.D., Lindo, S.,

874   Michael, S., Kuleshova, E., Ojala, D., et al. (2016). A Designer AAV Variant Permits

875   Efficient Retrograde Access to Projection Neurons. Neuron *92*, 372-382.

876   10.1016/j.neuron.2016.09.021.

877   35.   Zhang, Y., Wang, J., Li, J., Chen, Y., Sun, J., Lu, Z., Li, Y., and Liu, T. (2022). Functional

878   analysis of mutations endowing rAAV2-retro with retrograde tracing capacity. Neurosci

879   Lett *784*, 136746. 10.1016/j.neulet.2022.136746.

880   36.   Limberis, M.P., Vandenberghe, L.H., Zhang, L., Pickles, R.J., and Wilson, J.M. (2009).

881   Transduction efficiencies of novel AAV vectors in mouse airway epithelium in vivo and

882   human ciliated airway epithelium in vitro. Mol Ther *17*, 294-301. 10.1038/mt.2008.261.

883   37.   Halfmann, P.J., Iida, S., Iwatsuki-Horimoto, K., Maemura, T., Kiso, M., Scheaffer, S.M.,

884   Darling, T.L., Joshi, A., Loeber, S., Singh, G., et al. (2022). SARS-CoV-2 Omicron virus

885   causes attenuated disease in mice and hamsters. Nature *603*, 687-692.

886   10.1038/s41586-022-04441-6.

887   38.   Zhang, Y.N., Zhang, Z.R., Zhang, H.Q., Li, N., Zhang, Q.Y., Li, X.D., Deng, C.L., Deng,

888   F., Shen, S., Zhu, B., and Zhang, B. (2022). Different pathogenesis of SARS-CoV-2

889   Omicron variant in wild-type laboratory mice and hamsters. Signal Transduct Target

890   Ther *7*, 62. 10.1038/s41392-022-00930-2.

891   39.   Spitsin, S., Schnepp, B.C., Connell, M.J., Liu, T., Dang, C.M., Pappa, V., Tustin, R.,

892   Kinder, A., Johnson, P.R., and Douglas, S.D. (2020). Protection against SIV in Rhesus

893   Macaques Using Albumin and CD4-Based Vector-Mediated Gene Transfer. Molecular

894   therapy. Methods & clinical development *17*, 1088-1096. 10.1016/j.omtm.2020.04.019.

895   40.   Wang, D., Tai, P.W.L., and Gao, G. (2019). Adeno-associated virus vector as a platform

896   for gene therapy delivery. Nature Reviews Drug Discovery *18*, 358-378.

897   10.1038/s41573-019-0012-9.

898   41.   Mingozzi, F., and High, K.A. (2013). Immune responses to AAV vectors: overcoming

899   barriers to successful gene therapy. Blood *122*, 23-36. 10.1182/blood-2013-01-306647.

900   42.   Desch, A.N., Henson, P.M., and Jakubzick, C.V. (2013). Pulmonary dendritic cell

901   development and antigen acquisition. Immunol Res *55*, 178-186. 10.1007/s12026-012-

902   8359-6.

903   43.   Tosolini, A.P., and Sleigh, J.N. (2020). Intramuscular Delivery of Gene Therapy for

904   Targeting the Nervous System. Front Mol Neurosci *13*, 129. 10.3389/fnmol.2020.00129.

905   44.   Levin, M.J., Ustianowski, A., De Wit, S., Launay, O., Avila, M., Templeton, A., Yuan, Y.,

906   Seegobin, S., Ellery, A., Levinson, D.J., et al. (2022). Intramuscular AZD7442

907   (Tixagevimab-Cilgavimab) for Prevention of Covid-19. N Engl J Med.

908   10.1056/NEJMoa2116620.

909   45.   Miguez-Rey, E., Choi, D., Kim, S., Yoon, S., and Sandulescu, O. (2022). Monoclonal

910   antibody therapies in the management of SARS-CoV-2 infection. Expert Opin Investig

911   Drugs *31*, 41-58. 10.1080/13543784.2022.2030310.

912   46.   Sims, J.J., Lian, S., Meggersee, R.L., Kasimsetty, A., and Wilson, J.M. (2022). High

913   activity of an affinity-matured ACE2 decoy against Omicron SARS-CoV-2 and pre-

914   emergent coronaviruses. PLoS One *17*, e0271359. 10.1371/journal.pone.0271359.

915   47.   Tada, T., Norton, T.D., Leibowitz, R., and Landau, N.R. (2022). Directly injected lentiviral

916   vector-based T cell vaccine protects mice against acute and chronic viral infection. JCI

917   Insight. 10.1172/jci.insight.161598.

918   48.   Li, C., and Samulski, R.J. (2020). Engineering adeno-associated virus vectors for gene

919   therapy. Nat Rev Genet *21*, 255-272. 10.1038/s41576-019-0205-4.

920   49.   Martinez-Navio, J.M., Fuchs, S.P., Mendes, D.E., Rakasz, E.G., Gao, G., Lifson, J.D.,

921   and Desrosiers, R.C. (2020). Long-Term Delivery of an Anti-SIV Monoclonal Antibody

922   With AAV. Front Immunol *11*, 449. 10.3389/fimmu.2020.00449.

923   50.   Naso, M.F., Tomkowicz, B., Perry, W.L., 3rd, and Strohl, W.R. (2017). Adeno-Associated

924   Virus (AAV) as a Vector for Gene Therapy. BioDrugs *31*, 317-334. 10.1007/s40259-017-

925   0234-5.

926   51.   Wu, Z., Asokan, A., and Samulski, R.J. (2006). Adeno-associated virus serotypes: vector

927   toolkit for human gene therapy. Mol Ther *14*, 316-327. 10.1016/j.ymthe.2006.05.009.

928   52.   Weiss, A.R., Liguore, W.A., Domire, J.S., Button, D., and McBride, J.L. (2020). Intra-

929   striatal AAV2.retro administration leads to extensive retrograde transport in the rhesus

930   macaque brain: implications for disease modeling and therapeutic development. Sci Rep

931   *10*, 6970. 10.1038/s41598-020-63559-7.

932   53.   Sims, J.J., Greig, J.A., Michalson, K.T., Lian, S., Martino, R.A., Meggersee, R., Turner,

933   K.B., Nambiar, K., Dyer, C., Hinderer, C., et al. (2021). Intranasal gene therapy to

934   prevent infection by SARS-CoV-2 variants. PLoS Pathog *17*, e1009544.

935   10.1371/journal.ppat.1009544.

936   54.   Lana, M.G., and Strauss, B.E. (2020). Production of Lentivirus for the Establishment of

937   CAR-T Cells. Methods Mol Biol *2086*, 61-67. 10.1007/978-1-0716-0146-4_4.

938   55.   Lundstrom, K. (2021). Viral Vectors for COVID-19 Vaccine Development. Viruses *13*.

939   10.3390/v13020317.

940   56.   Ku, M.W., Authie, P., Nevo, F., Souque, P., Bourgine, M., Romano, M., Charneau, P.,
941   and Majlessi, L. (2021). Lentiviral vector induces high-quality memory T cells via
942   dendritic cells transduction. Commun Biol *4*, 713. 10.1038/s42003-021-02251-6.
943   57.   Kamath, A.T., Henri, S., Battye, F., Tough, D.F., and Shortman, K. (2002).
944   Developmental kinetics and lifespan of dendritic cells in mouse lymphoid organs. Blood
945   *100*, 1734-1741.
946   58.   van Furth, R. (1989). Origin and turnover of monocytes and macrophages. Curr Top
947   Pathol *79*, 125-150.
948   59.   Rawlins, E.L., and Hogan, B.L. (2008). Ciliated epithelial cell lifespan in the mouse
949   trachea and lung. Am J Physiol Lung Cell Mol Physiol *295*, L231-234.
950   10.1152/ajplung.90209.2008.
951   60.   Mehrabadi, A.Z., Ranjbar, R., Farzanehpour, M., Shahriary, A., Dorostkar, R.,
952   Hamidinejad, M.A., and Ghaleh, H.E.G. (2022). Therapeutic potential of CAR T cell in
953   malignancies: A scoping review. Biomed Pharmacother *146*, 112512.
954   10.1016/j.biopha.2021.112512.
955   61.   Mohanty, R., Chowdhury, C.R., Arega, S., Sen, P., Ganguly, P., and Ganguly, N. (2019).
956   CAR T cell therapy: A new era for cancer treatment (Review). Oncol Rep *42*, 2183-2195.
957   10.3892/or.2019.7335.
958   62.   Sterner, R.C., and Sterner, R.M. (2021). CAR-T cell therapy: current limitations and
959   potential strategies. Blood Cancer Journal *11*, 69. 10.1038/s41408-021-00459-7.
960   63.   Akerman, A., Milogiannakis, V., Jean, T., Esneu, C., Silva, M.R., Ison, T., Fitcher, C.,
961   Lopez, J.A., Chandra, D., Naing, Z., et al. (2022). Emergence and antibody evasion of
962   BQ and BA.2.75 SARS-CoV-2 sublineages in the face of maturing antibody breadth at

963   the population level. medRxiv, 2022.2012.2006.22283000.

964   10.1101/2022.12.06.22283000.

965 64.   Demogines, A., Farzan, M., and Sawyer, S.L. (2012). Evidence for ACE2-Utilizing

966   Coronaviruses (CoVs) Related to Severe Acute Respiratory Syndrome CoV in Bats.

967   Journal of Virology *86*, 6350-6353. 10.1128/jvi.00311-12.

968 65.   Wacharapluesadee, S., Tan, C.W., Maneeorn, P., Duengkae, P., Zhu, F., Joyjinda, Y.,

969   Kaewpom, T., Chia, W.N., Ampoot, W., Lim, B.L., et al. (2021). Evidence for SARS-CoV-

970   2 related coronaviruses circulating in bats and pangolins in Southeast Asia. Nature

971   Communications *12*, 972. 10.1038/s41467-021-21240-1.

972 66.   Aurnhammer, C., Haase, M., Muether, N., Hausl, M., Rauschhuber, C., Huber, I.,

973   Nitschko, H., Busch, U., Sing, A., Ehrhardt, A., and Baiker, A. (2012). Universal real-time

974   PCR for the detection and quantification of adeno-associated virus serotype 2-derived

975   inverted terminal repeat sequences. Hum Gene Ther Methods *23*, 18-28.

976   10.1089/hgtb.2011.034.

977 67.   Winkler, E.S., Bailey, A.L., Kafai, N.M., Nair, S., McCune, B.T., Yu, J., Fox, J.M., Chen,

978   R.E., Earnest, J.T., Keeler, S.P., et al. (2020). SARS-CoV-2 infection of human ACE2-

979   transgenic mice causes severe lung inflammation and impaired function. Nature

980   Immunology *21*, 1327-1335. 10.1038/s41590-020-0778-2.

981 68.   Corman, V.M., Landt, O., Kaiser, M., Molenkamp, R., Meijer, A., Chu, D.K., Bleicker, T.,

982   Brunink, S., Schneider, J., Schmidt, M.L., et al. (2020). Detection of 2019 novel

983   coronavirus (2019-nCoV) by real-time RT-PCR. Euro Surveill *25*. 10.2807/1560-

984   7917.ES.2020.25.3.2000045.

985
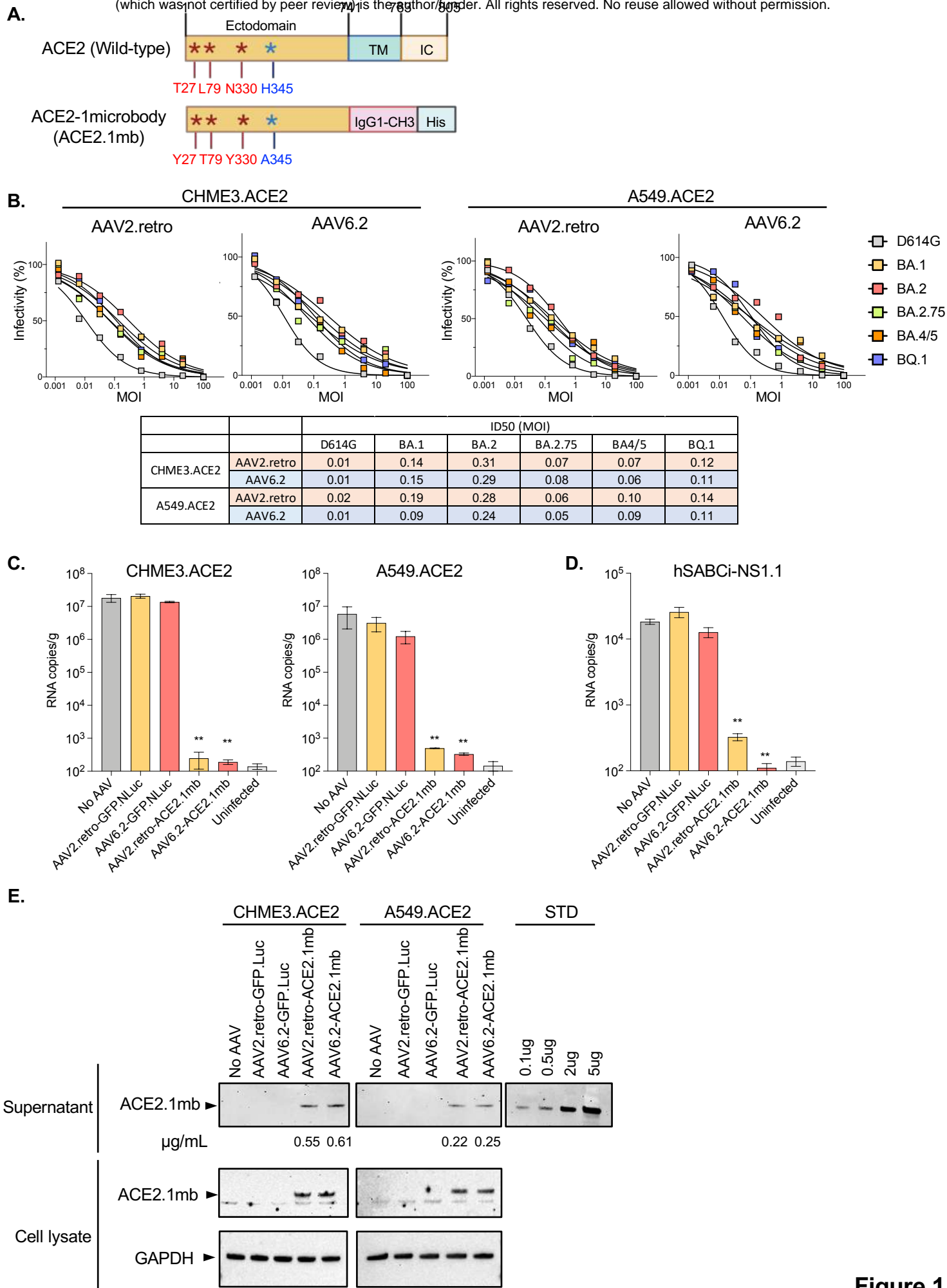
Figure 1
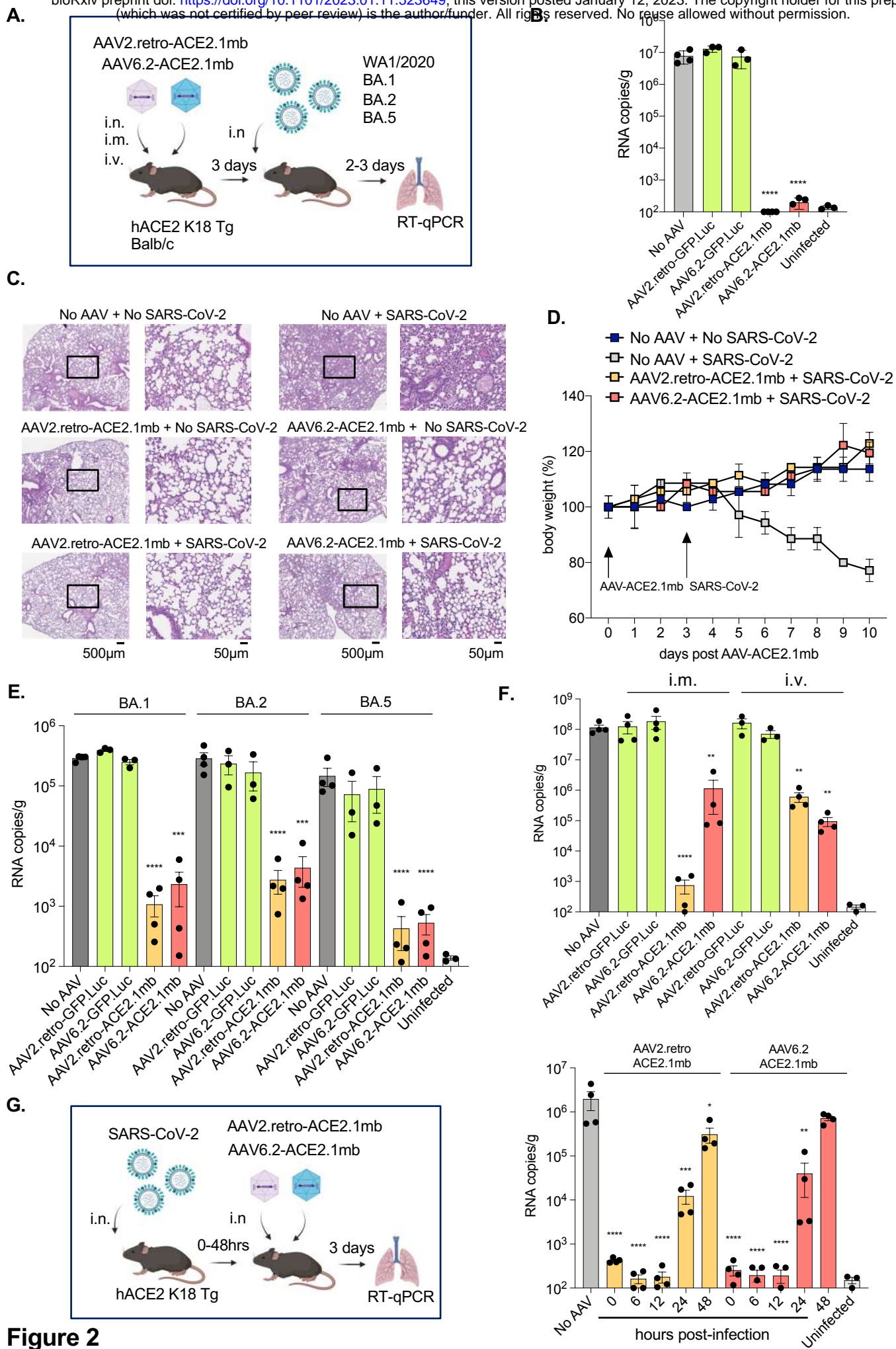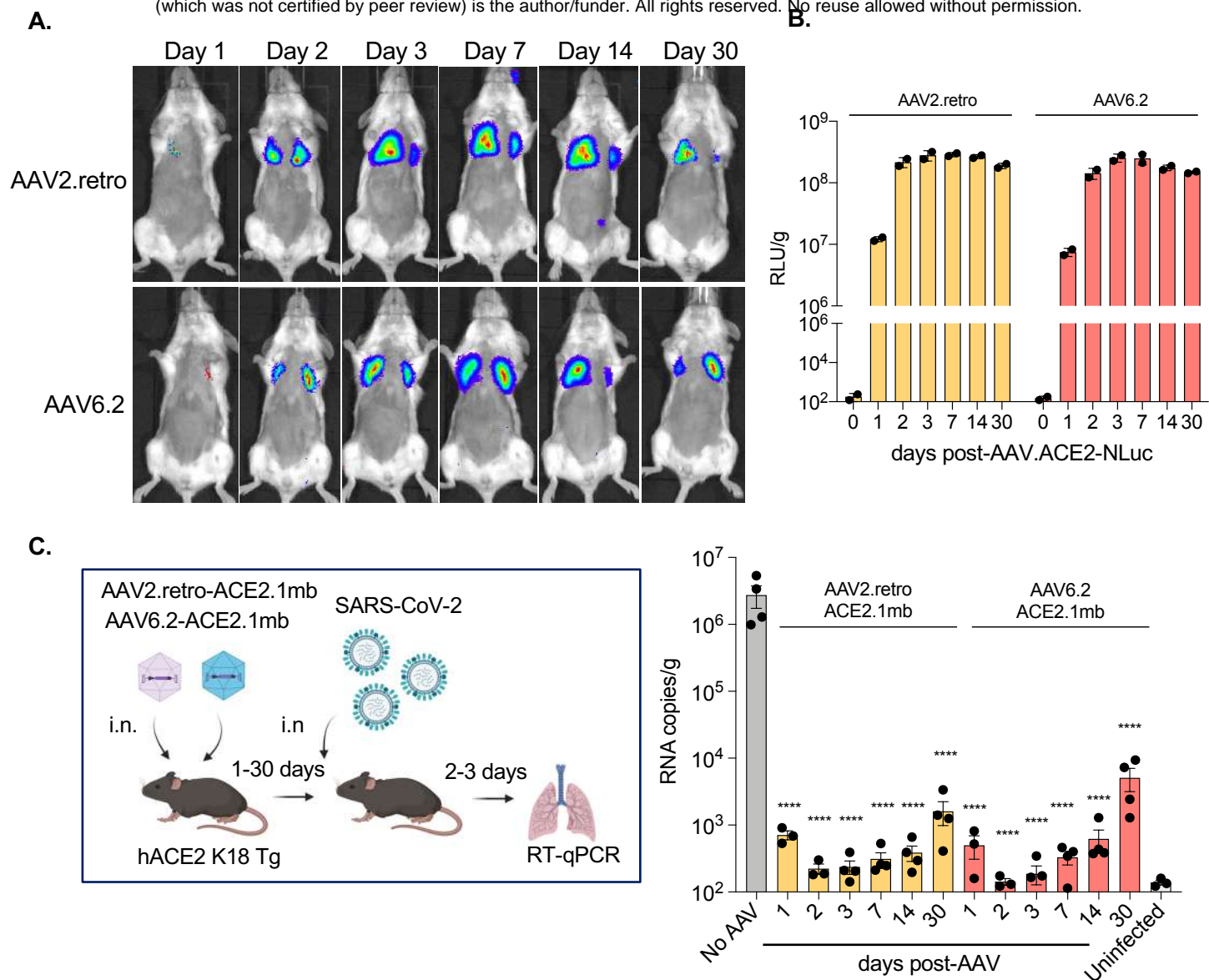
Figure 2

Figure 3

A.
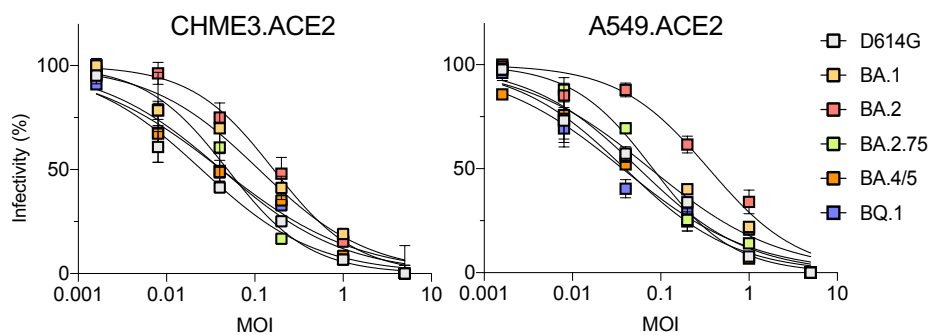
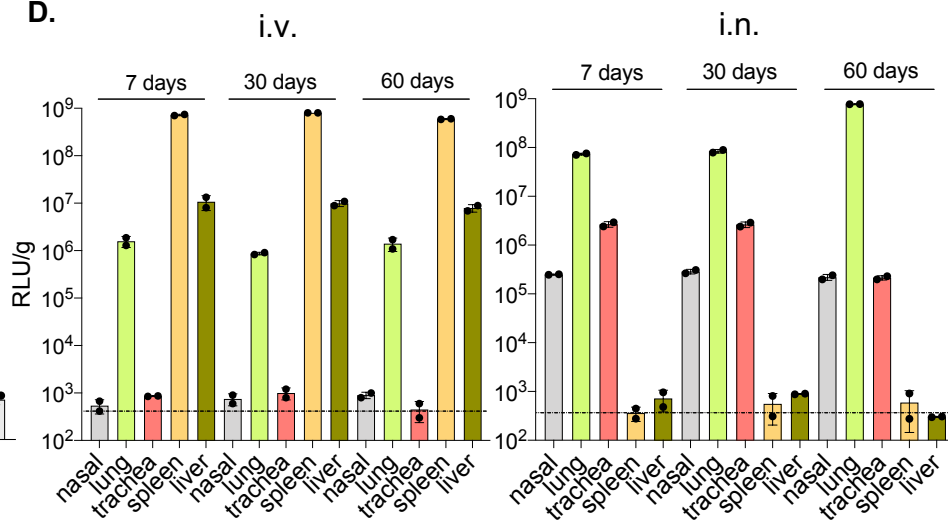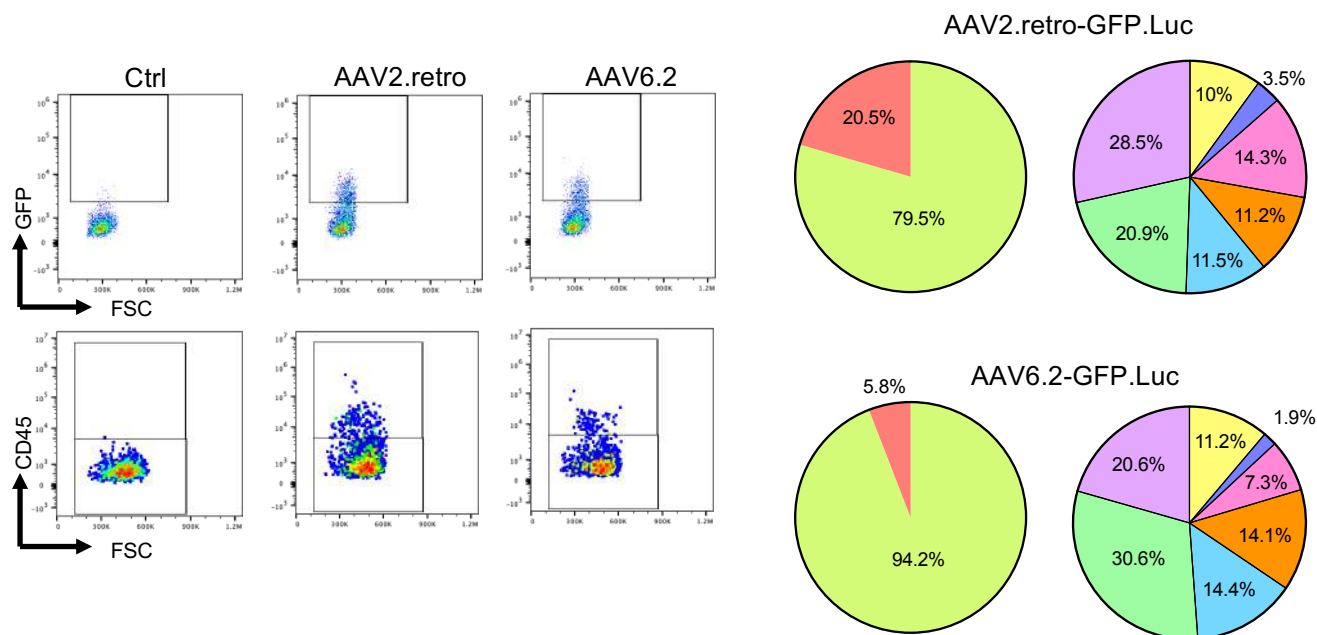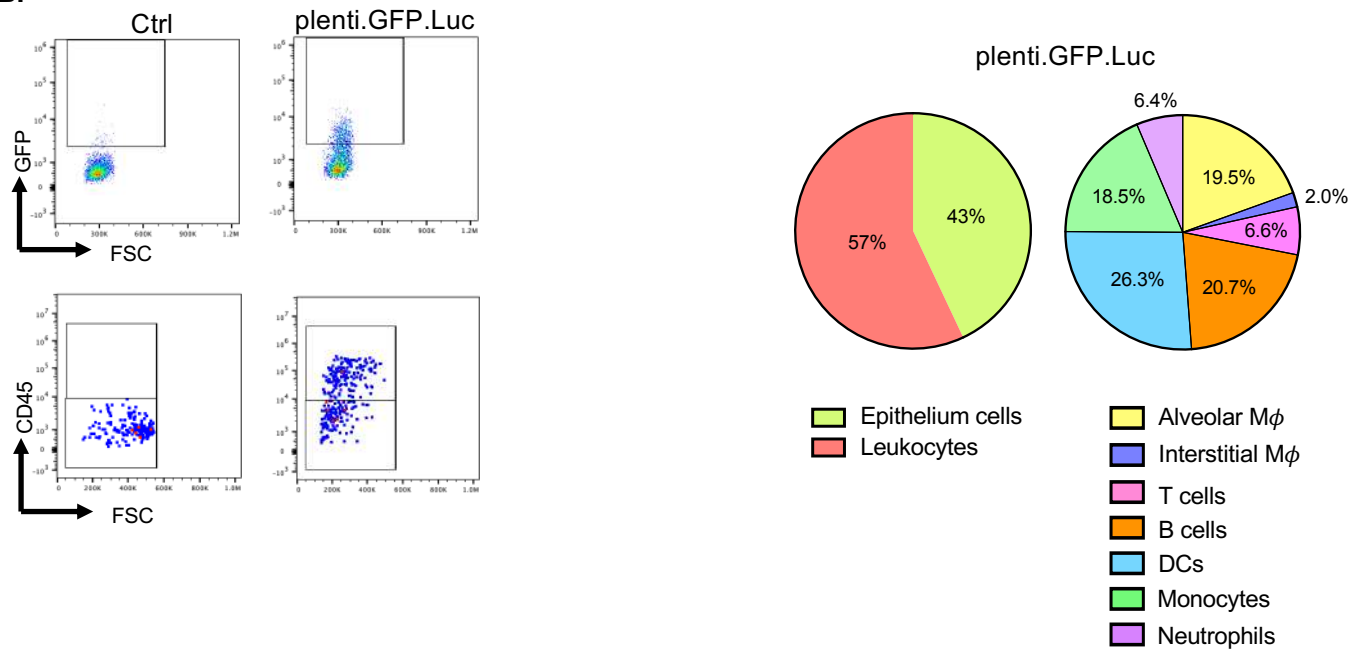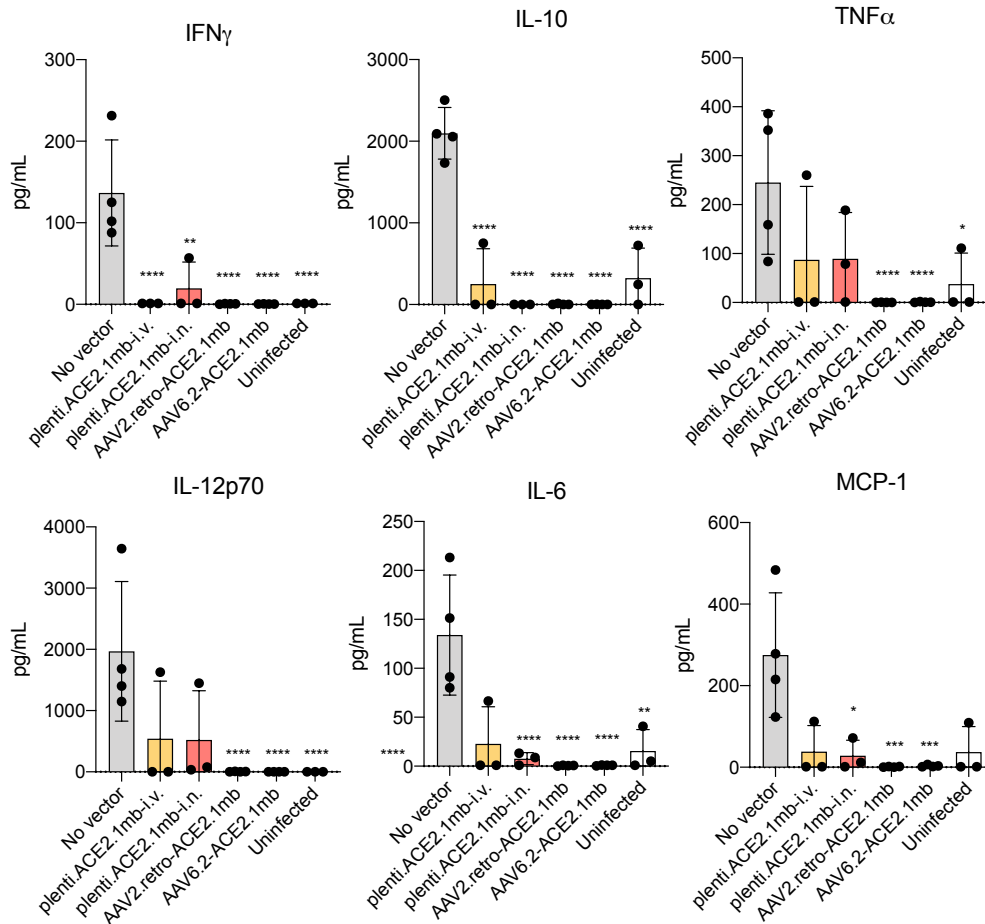|	ID50 (MOI)					
	D614G	BA.1	BA.2	BA.2.75	BA4/5	BQ.1
CHME3.ACE2	0.02	0.11	0.16	0.05	0.04	0.04
A549.ACE2	0.06	0.08	0.35	0.08	0.04	0.04

B.

C.

D.
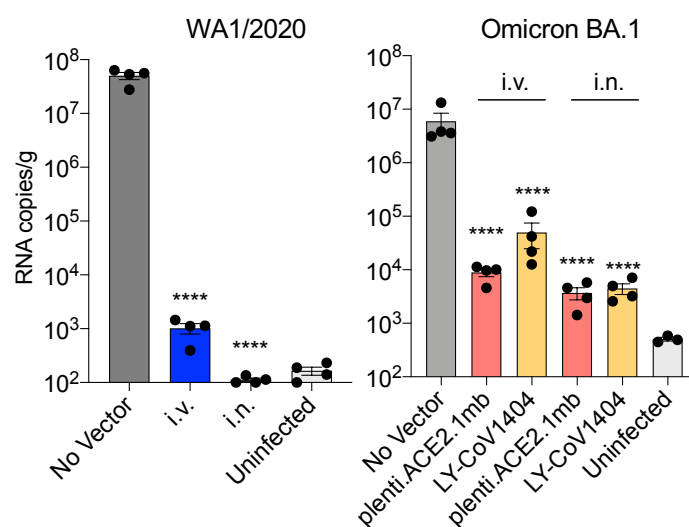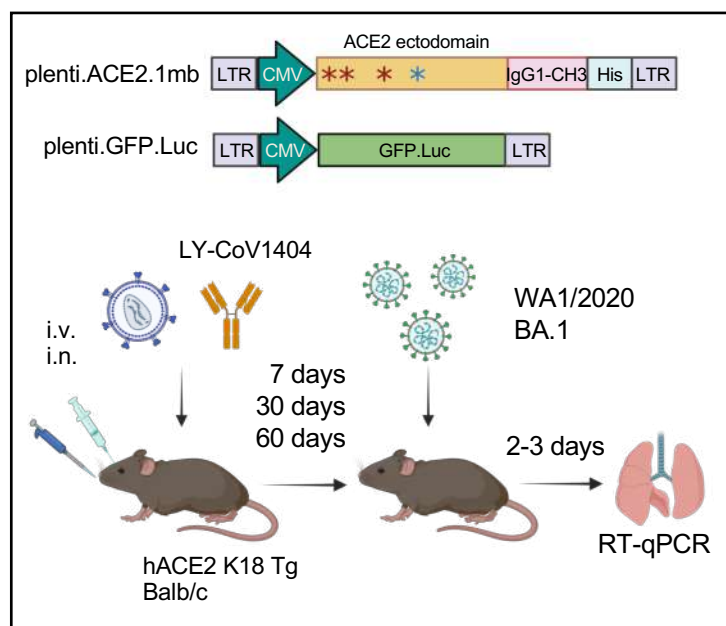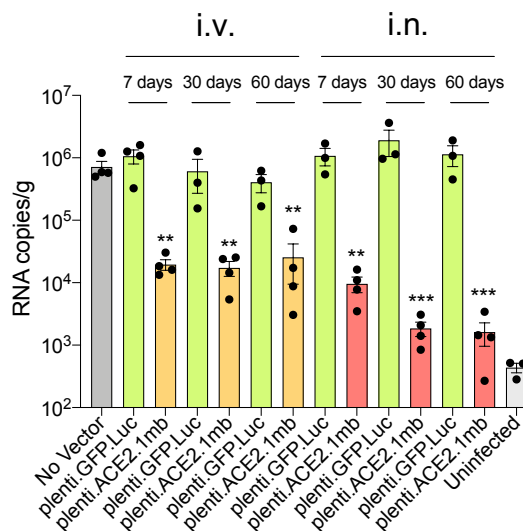
Figure 4

Figure 5

Figure S1. Intranasal injected AAV2.retro, AAV6.2-decoys and lentivirus-based ACE2.1mb didn't induce any inflammatory cytokine secretion.

Mice (n=4) were treated with the decoy-expressing AAV vectors (1 x 10^{12} IU) or decoy-expressing lentiviral vector (5 x 10^6 IU). After 3 (AAV) or 7days (lentiviral vector), the mice were challenged with SARS-CoV-2 WA1/2020 and 3-dpi the levels of IFNγ, TNFα, IL-10, IL-6, MCP-1 and IL-12p70 in lung were measured by cytokine beads array. The Y-axis shows the concentration of each cytokine. The experiment was done twice with similar results. Confidence intervals are shown as the mean ± SD. *P ≤ 0.05, **P ≤ 0.01, ***P≤0.001, ****P≤0.0001.

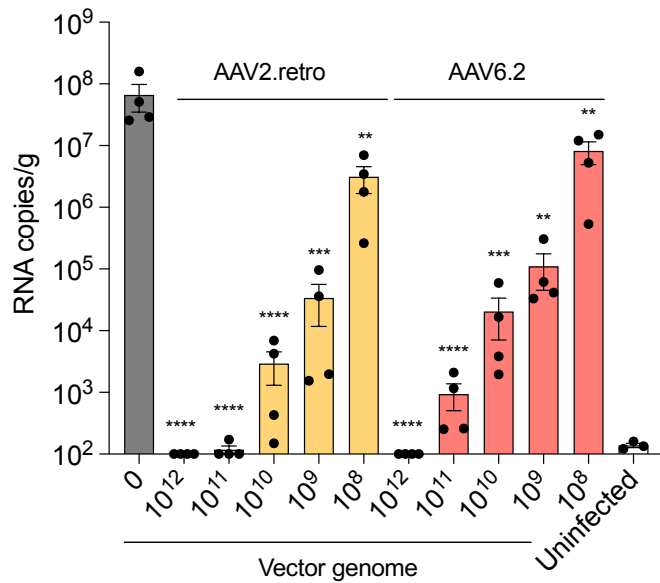**Figure S2. AAV-Decoy protected mice from SARS-CoV-2 infection.**

Different doses of decoy-expressing AAV vectors (1 X 10^{12}, 1 X 10^{11}, 1 X 10^{10}, 1 X 10^9, 1 X 10^8 vg) were administered to hACE2 K18 Tg (n=4) by i.n. instillation. 3 days post-AAV injection, mice were challenged with 1 X 10^4 PFU of SARS-CoV-2 WA1/2020. At 3-dpi, subgenomic viral E gene RNA in the lung were quantified. Confidence intervals are shown as the mean ± SD. **P ≤ 0.01, ***P≤0.001, ****P≤0.0001. The experiment was done twice with similar results.
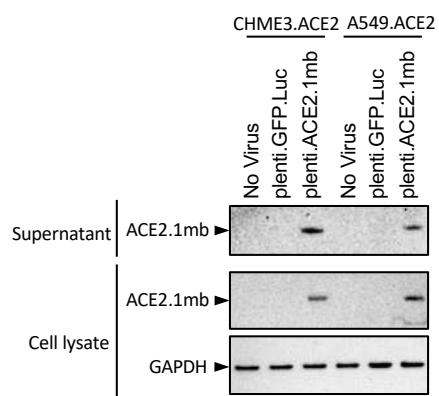
Figure S3. Lentivirus-based ACE2.1mb protected mice from SARS-CoV-2 infection.

CHME3.ACE2 and A549.ACE2 cells were transduced with decoy-expressing lentiviral vectors at an MOI of 0.5. 3-dpi, decoy protein secreted into the supernatant was pulled-down on NTA beads and bead-bound decoy protein was detected on an immunoblot probed with His-tag antibody. Decoy protein in the cell lysates is shown below with GAPDH as a loading control.
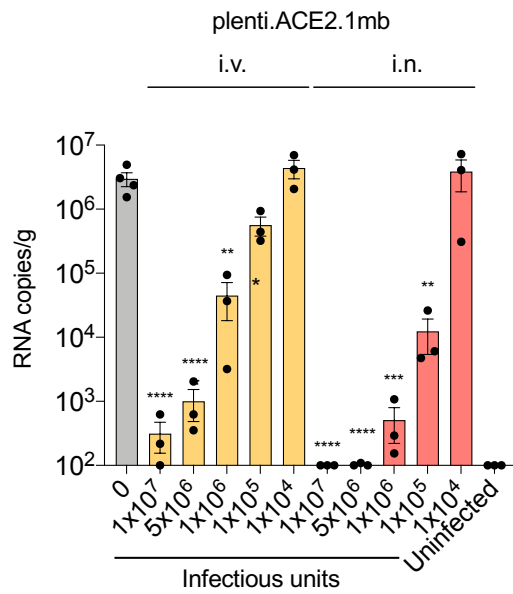
Figure S4. Lentivirus-based ACE2.1mb protect mice from SARS-CoV-2 infection.

hACE2 K18 Tg mice (n=3) were injected i.v. or i.n. with different amounts of decoy-expressing lentiviral vectors (1 X 10^7, 1 X 10^6, 1 X 10^5, 1 X 10^4 IU). One week later, the mice were challenged with 1 X 10^4 PFU SARS-COV-2. At 3-dpi, lung subgenomic viral E RNA was quantified by RT-PCR. Confidence intervals are shown as the mean ± SD. **P ≤ 0.01, ***P≤0.001, ****P≤0.0001.